An experimental study of the behavior of a model variable refrigerant flow system with common faults

Zhenxin Zhou[a] , Huanxin Chen[a,*], Lu Xing[b], Guannan Li[c], Wei Gou[a]

[a]Department of Refrigerant and Cryogenics Engineering, School of Energy and Power Engineering, Huazhong University of Science and Technology, Wuhan 430074, China

[b]Mechanical and Construction Engineering, Northumbria University, Newcastle upon Tyne, NE1 8ST, United Kingdom

[c]School of Urban Construction, Wuhan University of Science and Technology, Wuhan 430074, China

[*]Corresponding author:

Huanxin Chen, Department of Refrigeration and Cryogenic Engineering, school of Energy and Power Engineering, Huazhong University of Science and Technology

E-mail: chenhuanxin@tsinghua.org.cn

Tel.: +86-18971142396

ABSTRACT

Variable refrigerant flow (VRF) systems faults are inevitable due to installation errors, degradation, and other reasons. It is of great value to quantitatively understand the impact of faults on VRF systems performance and to clarify the changing trends of variables under different types of faults through experiments. In particular, the experimental analysis of simultaneous faults situations is helpful to improve the fault detection and diagnosis technology of VRF systems. There have been some previous experimental studies on the impact of faults, but none of them concerns modern VRF systems and their simultaneous faults. This paper presents results from a laboratory study of a VRF system with different types of faults. It provides the first published results of combinations of triple simultaneous faults, in addition to previously untested types of double simultaneous faults. The quantitative impact of the three crucial performance parameters, e.g. cooling capacity, system power, and COP, of the system under different faults has been analyzed. In addition, the quantitative influence and variation trend of system parameter variables during single fault and simultaneous fault are summarized. Results show that the outdoor fouling fault has the greatest impact, which can cause a 47.6% COP drop and 80.27% cooling capacity reduction. The influence of the simultaneous fault on

* Corresponding author.

E-mail: chenhuanxin@tsinghua.org.cn (H. Chen).

the variable trend is superimposed and offset, but the trend influence of some faults also has a dominant characteristic.

Keywords: Variable refrigerant flow system; Simultaneous faults; Fault impacts; Cooling Capacity

Nomenclature

COP	Coefficient of performance
FDD	Fault detection and diagnosis
HVAC	Heating ventilation and air conditioning
IF	Indoor units fouling
$Intensity_{OC/UC}$	Fault intensities of refrigerant overcharge or undercharge
$Intensity_{IF}$	Fault intensities of indoor fouling
$Intensity_{OF}$	Fault intensities of outdoor fouling
$Intensity_{NC}$	Fault intensities of non-condensable gas
OC	Refrigerant overcharge
OF	Outdoor unit fouling
UC	Refrigerant undercharge
VRF	Variable refrigerant flow
$A_{out.rated}$	The outdoor unit air inlet area
$A_{out.blocked}$	The blockage area
P_d	Compressor discharge pressure
P_s	Compressor suction pressure
$T_{\_suc}$	Compressor suction temperature
$T_{\_dis}$	Compressor discharge temperature
$T_{\_sc}$	Condenser supercooling temperature
$T_{\_sh}$	Discharge superheat temperature
$V_{in.air.rated}$	The standard indoor units air volume
$V_{in.air.decrease}$	The indoor units air volume decrease due to dirty blockage
$m_{ref.rated}$	The nominal refrigerant charge
$m_{ref.deviate}$	The overcharged or undercharged refrigerant charge amount
m_{NC}	The quality of the non-condensable gas
C	The air velocity
d	The diameter of tuyere
m	Quality
$\Phi_{(c)}$	Cooling capacity
q_{ml}	Indoor units air flow rate
$h_{air.in}$	Enthalpy of inlet air
$h_{air.out}$	Enthalpy of outlet air
V_n'	Specific volume of moist air
w_n	Air humidity ratio
W_{total}	Total power of system
ρ_v	The air density at the test point

1. Introduction

Building heating ventilation and air conditioning (HVAC) systems have significantly impact on the energy consumption of residential and commercial buildings. According to research in 2019[1], the energy consumption in building air conditioners accounts for more than 30% of the total residential electricity usage in China. Meanwhile, in the United States, the electricity use for residential space cooling was estimated to be 226 billion kWh in 2019[2]. Operating faults in the HVAC systems can reduce the system's performance and thus cannot maintain the user's thermal comfort needs under initial settings. Then the user had to change to a non-energy-saving setting to meet the demand, increasing energy required to cool buildings. To clarify the exact impact of these failures on the performance of the air-conditioning system is an essential step in the energy-saving assessment. The basis for air-conditioning system fault detection and diagnosis (FDD) is understanding the impact of faults on system parameter variables, such as temperatures and pressures. However, due to the complexity of the air-conditioning system, clearly understand the impact of faults on a specific type of system is an excellent choice through experiments to do[3, 4].

The research on the performance of the air-conditioning system by faults began in the 1990s. As of now, most of the research focuses on the experimental study of the single or double fault types of the air-conditioning system, and most of the research system objects are split system[5-9], rooftop unit[8, 10, 11], residential heat pump[12-15]. Refrigeration charge fault and heat exchanger fouling are the most concerned single fault type by research. The research on heat exchanger fouling can be traced back to 1987, in which Krafthefer et al.[16] estimated the impacts on COP for typical evaporator filter fouling of a heat pump. And then Bultman et al.[17] showed a 7.6% decrease in system COP for a 40% reduction in airflow for an air conditioner in 1995. The impact of fouling on plate-fin and spine-fin heat exchanger performance was also examined by Pak et al.[18] in 2005. The result shows that for the single-row heat exchangers, the pressure drop increased by 28 to 31%, while the heat transfer performance decreased by 7 to 12%. In 2008, Ali and Ismail[19] carried out experimental research to explore the effect on the performance of room air conditioners and impact on indoor air quality of evaporator air-side fouling. Qureshi and Zubair[20] performed fouling experiments in a vapor compression refrigeration system with a dedicated mechanical subcooling cycle in 2012. Immediately afterward, they obtained the impact in both system and performance parameters of fouling fault on the condenser of a vapor compression refrigeration system by an experimental observation[21]. According to the numerical value of the relative standard charge, refrigeration charge fault can be divided into refrigerant undercharge (UC) and refrigerant overcharge (OC). As the heat transfer carrier, refrigerant can significantly impact the system, whether it is overcharged or undercharged, so the attention of this fault can also be traced back to the early 1990s. The typical representatives of this period are the research of Farzad[6] and Bailey[22]. Then, with the renewal and iteration of the air-conditioning system, some scholars carried out further research on the new system. In 2005, Grace et al.[23] presents results of experimental investigations on the effect of refrigerant charge fault in vapor compression refrigeration systems. The impact of refrigerant charge faults on single-speed air-cooled air-conditioners and heat pumps was summarized by Mehrabi and Yuill[24] in 2017. Very few studies have investigated non-condensable gas (NC) fault, because of its extremely high safety requirements

for experiments. However, the NC fault is easy to cause due to irregular installation operations. From the public literature, only four experiments involve NC faults [15], and its research objects are rooftop air conditioners and residential heat pump systems.

With the deepening of research, few researchers also began to comprehensively analyze system faults, considering multiple fault types and simultaneous faults. Du et al.[8] experimented common faults (refrigerant undercharge/overcharge, evaporator low indoor airflow and condenser low outdoor airflow) on split and rooftop system. Hu et al.[15] conducted experimental research on common installation faults in a high-efficiency residential heat pump. The four types of faults considered in the paper are improper evaporator airflow rate, refrigerant undercharge or overcharge, liquid line restriction, and non-condensable gas. After that, Hu et al.[25] also researched the simultaneous faults composed of these single faults.

Through literature analysis, the following research status can be summarized:

(1) The most common types of faults that affect the performance of the air conditioning system are: refrigerant undercharge (UC), refrigerant overcharge (OC), indoor units fouling (IF), outdoor unit fouling (OF), and non-condensable gas in the refrigerant (NC). Among them, there are more studies on the first four categories, and NC faults are less studied due to the high safety requirements of their experiments.

(2) Most experiments only analyze the impact of one or two system fault types on performance due to the experiment's immense workload and stringent requirements. There are few works on experiments on the general fault of the system, while it is of great significance for the macro consideration of the impact of failures and comparing the effect of different fault types on the system.

(3) There is even less research on simultaneous fault studies as experiments and analysis are more complex. But in actual situations, simultaneous faults are inevitable. Carrying out simultaneous fault experiments has a realistic background and practical significance.

(4) There are few fault experiments on frequency-conversional VRF systems. The cost of destructive fault experiments is high due to the high system selling price, and the fault experiments are complicated, and the experiment requirements are high. In addition, there is almost no public literature involved in VRF system simultaneous fault impacts analysis.

The VRF systems, which provide a more comfortable and stable indoor thermal environment and reduce cooling energy consumption, have been increasingly applied for buildings such as commercial buildings, office rooms, and et.al[26]. In addition, it is relatively simple to set up and install by reducing the need for ductwork installation. According to a research report[27], the global VRF systems market to reach $29 Billion by 2027 and at the same time, China is forecast to reach a projected market size of $6.4 Billion. VRF systems faults are inevitable due to installation errors, degradation due to operation and other reasons[28]. Unfortunately, there are research gaps in analyzing the fault impact on VRF system, which occupies an important position in the air conditioning system. To address research gaps, this paper conducts experimental research on five common fault types. It analyzes the performance impact and variables variation trend of VRF systems under three faults sit: single faults, double simultaneous faults, and triple simultaneous faults. The core contribution of this study has three points:

(1) This paper provides a comprehensive reference database of the impact of fault on the frequency conversional VRF system, filling the research gap that the reference database is missing.
(2) The paper profoundly analyzes the influence of multiple faults and multiple fault levels of VRF systems on system performance. It explores the actual performance influence degree of simultaneous faults (double-simultaneous, triple-simultaneous) and internal mutual coupling influence law for the first time.
(3) The paper deeply analyzes the trend influence of single fault and simultaneous faults on characteristic variables and explores the interaction between fault impacts on variables under simultaneous faults; it can guide FDD models' development.

The current paper demonstrates a great experimental effort to solve critical problems involving common single-faults and corresponding simultaneous faults in VRF systems. The rest of paper is organized as follows: Section 2 describes methods for imposing and combining faults in the laboratory, and metrics to describe the fault impacts. According to the complexity of the faults, Section 3 analyzes the impact of single faults, double simultaneous faults, and three simultaneous faults on the VRF system. Section 3.1 to Section 3.3 summarizes the quantitative impacts of various types of faults and provides some methods and an analysis to address the problem of simultaneous faults. And then, Section 3.4 analyzes and summarizes the quantitative influence and variation trend of system parameter variables during single fault and simultaneous fault, which guides for the problem of fault decoupling when developing VRF system FDD tools. Finally, the last section provides a conclusive summary of the results.

2. Experimental setup and faults introduction

The experimental conditions are standard cooling conditions, i.e. indoor Dry-bub temperature 27℃ (Wet-bub temperature 19℃) and outdoor Dry-bub temperature 35℃. This section describes experiments to test these faults singly and simultaneous, including a detailed description of the test setup, instrumentation, fault implementation, and evaluation index.

2.1 Psychrometric chamber

All the experiments were performed in a standard psychrometric chamber to tightly control the indoor and outdoor air dry-bulb and wet-bulb temperatures. The standard psychrometric chamber is composed of a 50HP outdoor chamber and a 30HP indoor chamber. There is a set of air volume devices in the indoor chamber with an air volume range of 500-10000m³/h, which adopts independent measurement and control methods to make the inlet temperature measurement accurate. This standard psychrometric chamber adopts the theory of air enthalpy potential, which uses the indoor air-side enthalpy method to measure the room air conditioner's cooling (heat) quantity. It is designed and built according to the following national standards of China: GB/T18837-2015, GB/T19409-2003, GB/T18430.2-2008, GB/T18430.1-2007, GB/T7725-2004, GB/T17758-2010, GB/T18836-2002, GB/T19232-2003. These standards can be found in the website[29]: http://www.cssn.net.cn/pagesnew/search/search_base_EN.jsp.

During the test, the standard psychrometric chamber can guarantee that the indoor and outdoor chamber's return air temperature deviation was less than 0.5℃ and 1℃, respectively. The main

measuring instruments and their accuracy of the standard psychrometric chamber are shown in **Table 1**. The laboratory is equipped with a Yokogawa MW100 data collector. Corresponding sensors are arranged according to the performance test requirements, and then the data is integrated by ACTest soft, and the superheat and supercool calculations are performed. During the experiment, the data collection interval was set at ten seconds. The following experiment guidelines are carried out as required before each experiment: 1) Check the last operation record to confirm whether the equipment is faulty, if there is a fault, confirm that the fault has been eliminated, and the equipment is normal before it is ready to start up; 2) Check whether the power supply is normal; 3) Fill the water bottle on the temperature measuring device with distilled water, change the wet-bulb gauze every 48 hours and keep the platinum resistance wet-bulb thermometer about 28±2mm away from the water surface; 4) Detect the sealing condition of all interfaces; 5) According to the air volume of the tested machine, select the appropriate number of the nozzle so that the nozzle wind speed is between 20~30m/s.

Table 1 The measuring accuracy of the sensors.

Sensor	Range	Accuracy	Measurement location
T-type thermocouples	-200~350 ℃	±0.5 ℃	Refrigerant
Platinum-resistance thermocouple	-200~500 ℃	±0.1 ℃	Air
Relative humidity sensor	0~98%	±5% RH	Air
Pressure transducer	-0.1~5 MPa	±0.2%	Refrigerant
Pressure transducer	0-1000 Pa	±0.2%	Air in the wind chamber
Power meter	0.5~100 kHz	±0.2% FS	Indoor and outdoor testing rooms

2.2 Experimental apparatus

A scheme of the experimental VRF system is shown in **Fig. 2**. The test system is a nominal 15.5 kW VRF system with R410A refrigerant, with a standard charge of 6.3 kg. It is composed of five indoor units and one outdoor unit. The rated cooling capacity of the five indoor units are 2.2kW, 2.8kW, 2.8kW 3.6kW, and 7.1kW. **Table 2** presents detail information about the indoor units. The diameter of the liquid pipe is 6.35mm and the length is 20m. The diameter of the trachea is 9.53mm and the length is 30m. In cooling operation, its environmental operating range is 10℃ to 46℃, and in heating, the range is -20℃ to 15.5℃. The outdoor unit comprised an inverter two-spool compressor, four-way valve, gas-liquid separator, fin-tube heat exchangers, outdoor electronic expansion valve (EEV), check valve and bypass solenoid valve.

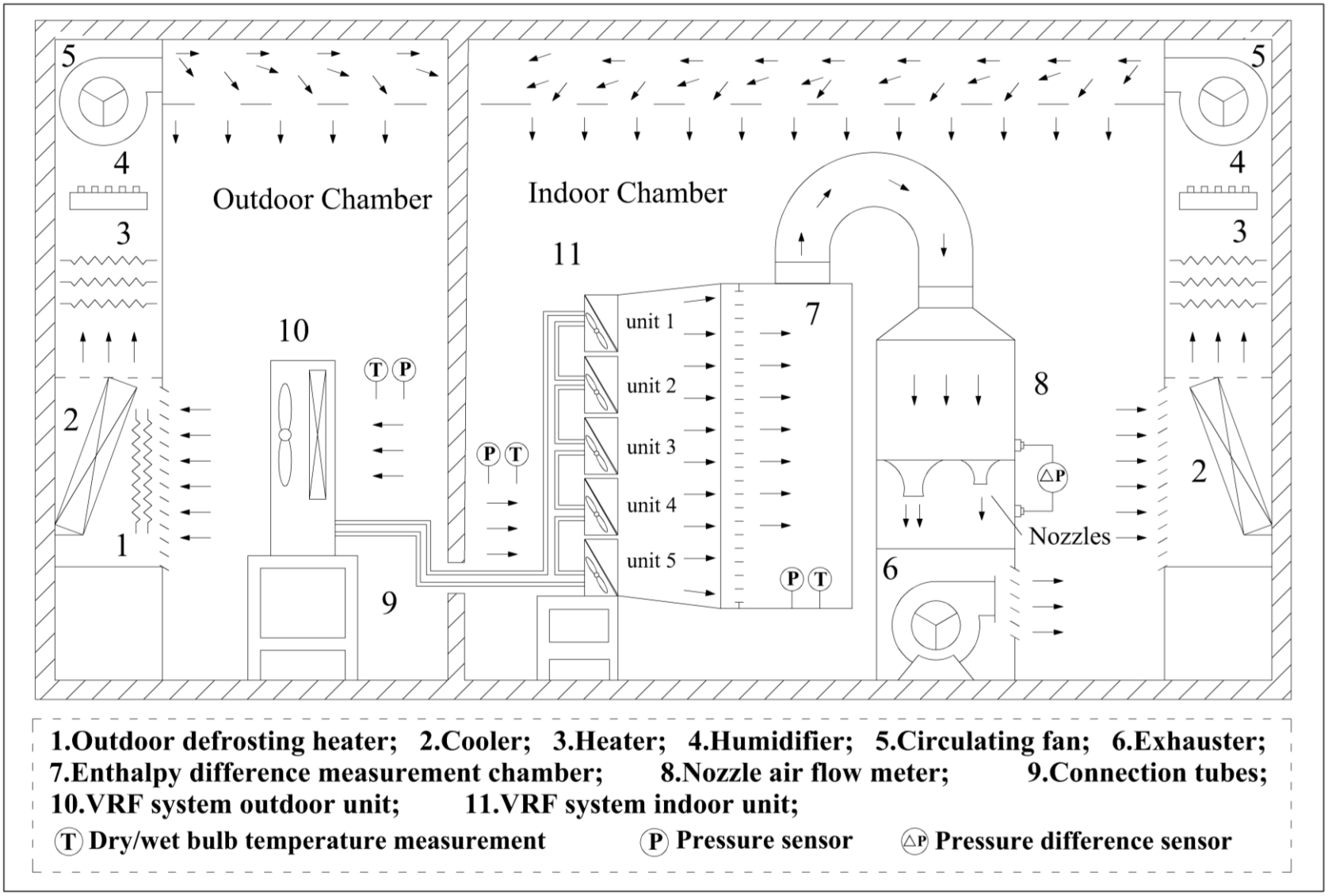

Fig.1 The schematic diagram of the standard psychrometric chamber

The inverter two-spool compressor serves as the power source for the heat transfer of the VRF system, and its standard operating pressure ratio ranges from 1.6 to 10. It required operating conditions range from the evaporation temperature between -27 and 26℃ (i.e., 0.20~1.60MPa), and the condensation temperature between -15 and 65℃ (i.e., 0.38~4.15MPa). VRF systems need to meet heating and cooling requirements, and four-way valves realize this function. It changes the flow path of refrigerants by controlling the pilot valve to switch the mode between cooling and heating. The gas-liquid separator is used to separate liquid and gaseous refrigerants to avoid liquid shock in the compressor. The outdoor heat exchanger is the core device to realize heat transfer. The refrigerant flow rate can be adjusted by the opening ratio of the EEV, while under the cooling model, the opening ratio of the outdoor EEV remains 100%. The amount of refrigerant flowing through the unit was adjusted by the compressor rotation frequency and the indoor EEV opening ratio, at this time.

Table 2. Indoor units' parameters information

Parameters	Indoor unit 22	Indoor unit 28	Indoor unit 36	Indoor unit 71
Size (H×W×D) mm		192×700×447		192×1180×447
Air flow rate (m^3/min)	7.3	9	9	16.5
Net weight (kg)	16	17	17	24
Cooling capacity (kW)	2.2	2.8	3.6	7.1
Heating capacity (kW)	2.5	3.2	4.0	8.0
Cooling rated input (kW)	0.03	0.04	0.04	0.06
Heating rated input (kW)	0.03	0.04	0.04	0.06
Cooling rated current (A)	0.25	0.35	0.35	0.50
Heating rated current (A)	0.25	0.35	0.35	0.50

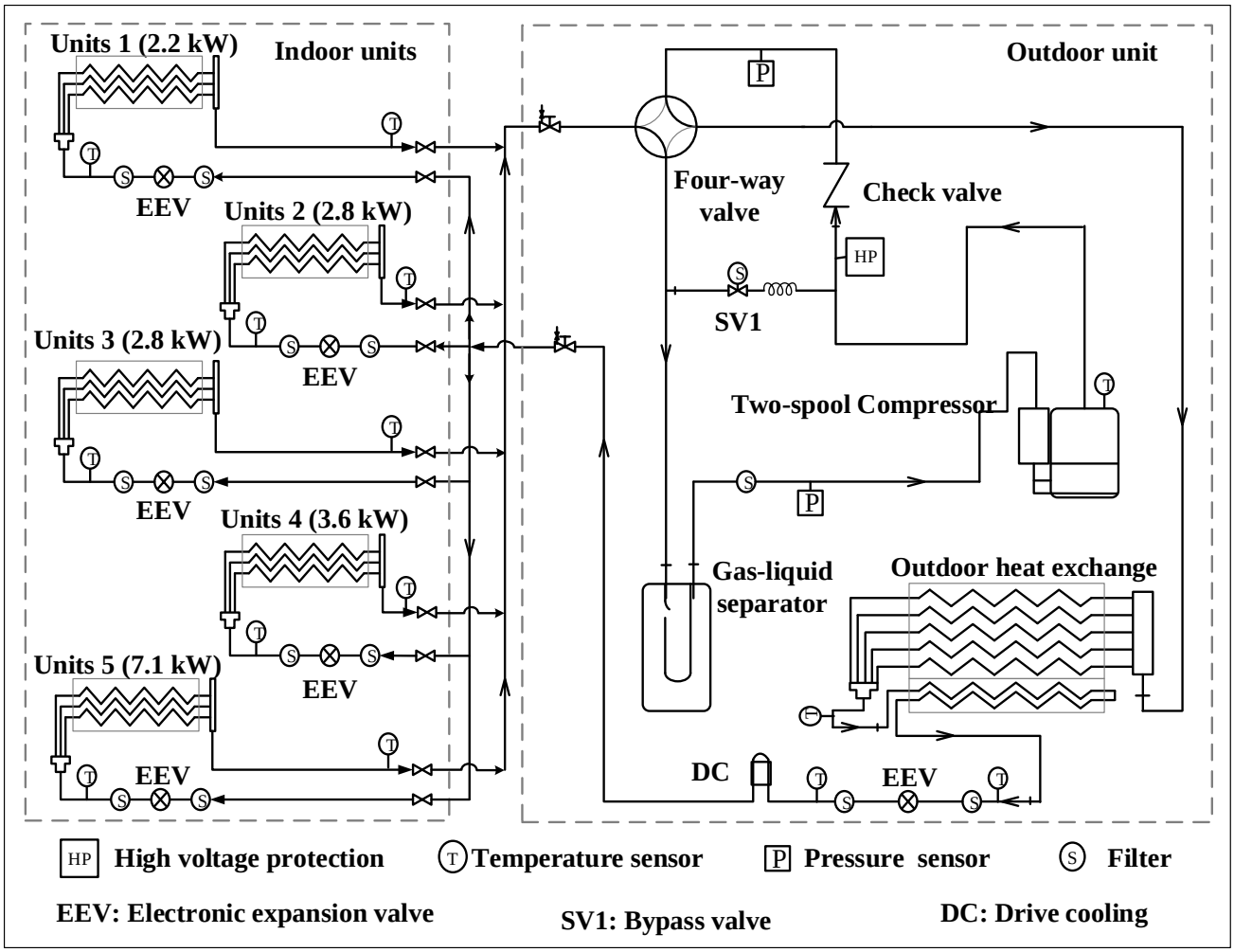

Fig.2. The schematic diagram of the VRF system

2.3 Fault description

Five fault types and their corresponding simultaneous fault were selected because they represent all the common faults during installation and operation. They are refrigeration overcharge (OC), refrigeration undercharge (UC), outdoor unit fouling (OU), indoor units fouling (IU), and non-condensable gas (NC). Since non-condensable gas may cause an explosion in the system, it wasn't carried out in the simultaneous fault experiment after considering safety. **Table 3** shows the detailed test matrix information.

The refrigerant serves as a "medium" for heat transfer, and its change level will significantly impact the VRF system. In the experiment, the "weighing method" is used to achieve different refrigerant charging levels. The nominal charge is 6.3 kg based on the manufacturer's charging instructions. The definition of fault intensities is shown in **Eq. (1)**[15].

$$Intensity_{OC/UC} = \frac{m_{ref.actual}}{m_{ref.rated}} \tag{1}$$

Where $m_{ref.rated}$ indicates the nominal refrigerant charge, $m_{ref.actual}$ indicates the actual refrigerant charge.

Due to aging, or being covered by dust, or obstruction of heat dissipation and ventilation, the heat exchange performance of the condenser and evaporator will reduce. For indoor units, their air inlets are blocked to reduce their air volume, thereby setting different levels of indoor fouling. The definition of indoor fouling intensity is shown in **Eq. (2)**[8].

$$Intensity_{IF} = \frac{V_{in.air.decrease}}{V_{in.air.rated}} \tag{2}$$

Where $V_{in.air.rated}$ indicates the standard air volume, $V_{in.air.decrease}$ indicates the air volume decrease due to dirty blockage.

The outdoor fouling is similar, but the fouling intensity is defined as the ratio of the blocked area of the air inlet of the outdoor unit to the total area. The definition of outdoor fouling intensity is shown in **Eq. (3)**[30].

$$Intensity_{OF} = \frac{A_{out.blocked}}{A_{out.rated}} \tag{3}$$

Where $A_{out.rated}$ indicates the outdoor unit air inlet area, $A_{out.blocked}$ indicates the blockage area.

The non-condensable gas is mainly because the installation process is not vacuumed according to the standard manual. The fault intensity is mainly determined by the quality of the non-condensable gas contained in the system. The mixing of non-condensable gases will cause safety hazards to the system. Not only will it reduce the performance of the VRF system, but it will also cause an explosion in severe cases. Therefore, only three groups of single faults were conducted in the experiment. The definition of non-condensable gas fault intensity is shown in **Eq. (4)**[15]. m_{NC} indicates the quality of the non-condensable gas.

$$Intensity_{NC} = m_{NC} \tag{4}$$

It is reasonable to assume that faults often do not appear alone, but are mutually associated, because faults often result from low-quality installation or a lack of maintenance and harsh operating conditions[25]. When the system has a refrigeration charge fault, it is possible to superimpose other faults (e.g., OF, IF). Therefore, this paper considers the double simultaneous faults and triple simultaneous, which is common in the system. In addition, because different fault intensities will cause different impacts on the system, we also comprehensively considered the superposition of varying fault intensities in the simultaneous faults experiment. The following paper and figures use a "+" symbol to represent the fault superimpose. For instance, "UC80+OF50" represents the simultaneous fault of the refrigerant undercharge fault intensity 80% with outdoor fouling fault intensity 50%.

Table 3. Test matrix for selected single faults and their corresponding simultaneous faults

Fault types	Abbreviation	Description	Intensities
		Single fault	
Refrigerant overcharge	OC	The refrigerant charge of the system exceeds the standard charge by more than 10%	110%, 120% 130%, 140%
Refrigerant undercharge	UC	The refrigerant charge of the system is more than 10% lower than the standard charge	90%, 80% 70%,60%,50%

Indoor unit fouling	IF	The heat exchange performance of the indoor heat exchanger is reduced by airflow rate	25%,50%,75%
Outdoor unit fouling	OF	The heat exchange performance of the outdoor heat exchanger is reduced by airflow rate	25%, 50%, 75%, 100%
Non-condensable gas	NC	The system contains non-condensable gas	10g, 20g, 50g
Double simultaneous fault			
Indoor units fouling with refrigerant charge fault	IF+OC/UC	The system has double faults indoor units fouling and refrigerant charge fault at the same time	IF50+OC120 IF50+UC80
Indoor units fouling with outdoor unit fouling	IF+OF	The system has double faults indoor units fouling and outdoor unit fouling at the same time	IF50+OF25 IF50+OF50 IF50+OF75
Refrigerant overcharge with outdoor unit fouling	OC+OF	The system has double faults refrigerant overcharge and outdoor unit fouling at the same time	OC120+OF50 OC120+OF75
Refrigerant undercharge with outdoor unit fouling	UC+OF	The system has double faults refrigerant undercharge and outdoor unit fouling at the same time	UC80+OF50 UC80+OF75
Triple simultaneous fault			
Refrigerant overcharge, indoor units fouling with outdoor unit fouling	OC+IF+OF	The system has triple faults refrigerant overcharge, indoor units fouling with outdoor unit fouling at the same time	OC120+IF50+OF50 OC120+IF50+OF75
Refrigerant undercharge, indoor units fouling with outdoor unit fouling	UC+IF+OF	The system has triple faults refrigerant undercharge, indoor units fouling with outdoor unit fouling at the same time	UC80+IF50+OF50 UC80+IF50+OF75

2.4 Evaluation index

The paper uses the cooling capacity, the total power of the system, and coefficient of performance (COP) to evaluate the performance of the VRF system. Their calculations are based on the literature[31]. The experiment uses the indoor air-side enthalpy method to measure the cooling quantity of the test VRF system. The cooling capacity $\Phi_{(c)}$ was calculated by the following **Eq. (5)**.

$$\Phi_{(c)} = \frac{q_{ml}(h_{air.in} - h_{air.out})}{V_n'(1 + w_n)} \quad (5)$$

Where $\Phi_{(c)}$ was the cooling capacity of test VRF system. q_{ml}, $h_{air.in}$, $h_{air.out}$, V_n', w_n denoted the indoor units air flow rate (m^3/s), enthalpy of inlet air ($J/kg_{dry.air}$), enthalpy of outlet air($J/kg_{dry.air}$), specific volume of moist air (m^3/kg) which can be calculated by **Eq. (6)** and air humidity ratio ($kg/kg_{dry.air}$) which equation is shown in **Eq. (7)**, respectively.

$$V_n' = \frac{0.455(0.622 + w_n)(T_w + 273.15)}{9.869 \times 10^{-4}(1 + w_n)P} \tag{6}$$

$$w_n = \left(\frac{\varphi p}{P - \varphi p}\right) \tag{7}$$

None of these five variables can be directly measured, and they need to be measured indirectly through the measured values the inlet temperature, the inlet air wet-bulb temperature, the outlet temperature, outlet air wet-bulb temperature and so on. The q_{ml} can be calculated by **Eq. (8)**

$$q_{ml} = C * A * \sqrt{2\rho_v V_n'} = C * \pi * \frac{d^2}{4} * \sqrt{2\rho_v V_n'} \tag{8}$$

Where C was the air velocity (m/s); ρ_v was the air density at the test point; d was the diameter of tuyere.

The $h_{air.in}$ can be obtained from temperature and humidity, as shown in **Eq. (9)**. The same can also be calculated to obtain $h_{air.out}$.

$$h_{air.in} = f(T_{air.in}, WB_{air.in}, P_{air.in}) = 1.005t_{in} + w_{n\_in}(2500 + 1.84t_{in}) \tag{9}$$

The total power W_{total} of the system can be directly collected by the power meter. Therefore, the system COP can be calculated by **Eq. (10)**.

$$COP = \frac{\Phi_{(c)}}{W_{total}} \tag{10}$$

2.5 Uncertainty analysis

Measurement uncertainty is an important index to evaluate the measurement quality and data reliability of a measurement system. To assess the credibility of the collected data of the test VRF system, this section calculates the uncertainty of the important measurement data such as the cooling capacity and COP of the air-side enthalpy potential method according to the standard JJF1059-1999.In the air-side enthalpy potential method, the cooling capacity of the VRF system is calculated by the **Eq. (5)**. According to the uncertainty transfer formula of the indirect measurement (National Bureau of Quality and Technical Supervision of China, 1999), the standard uncertainty of the indoor cooling capacity can be calculated according to **Eq. (11)**.

$$\begin{aligned} u_{Q_c}^2 = {} & \left[\frac{h_{a1} - h_{a2}}{V_n(1 + W_n)}\right]^2 u_{q_f}^2 + \left[\frac{q_f}{V_n(1 + W_n)}\right]^2 \left(u_{h_{a1}}^2 + u_{h_{a2}}^2\right) \\ & + \left[\frac{q_f(h_{a1} - h_{a2})}{(V_n)^2(1 + W_n)}\right]^2 u_{V_n}^2 + \left[\frac{q_f(h_{a1} - h_{a2})}{V_n(1 + W_n)^2}\right]^2 u_{W_n}^2 \\ & = c_1^2 u_{q_f}^2 + c_2^2\left(u_{h_{a1}}^2 + u_{h_{a2}}^2\right) + c_3^2 u_{V_n}^2 + c_4^2 u_{W_n}^2 \end{aligned} \tag{11}$$

Where $u_{Q_c}^2$ was the uncertainty of cooling capacity; $u_{q_f}^2$ and c_1^2 are the uncertainty and the its transfer coefficient of the air volume flow; $u_{h_{a1}}^2$, $u_{h_{a2}}^2$ and c_2^2 are the uncertainty of the air enthalpy value and its transfer coefficient; $u_{V_n}^2$ and c_3^2 are the uncertainty of the air specific volume and its transfer coefficient; $u_{W_n}^2$ and c_4^2 are the uncertainty of the air specific volume and its transfer coefficient.

The measurement uncertainty of the basic sensor can be obtained from **Table 1**, and substituting **Eq. (11)** to obtain the uncertainty range of u_{Qc} is 0.7% ~ 1.6%. Besides, the uncertainty range of the measured power was calculated according to the test value of power and the maximum error of power meter in 0.6% ~ 1.4%. In the same way, according to **Eq. (10)** and u_{Qc}, the uncertainty range of the COP can be calculated in 0.8% ~ 1.7%. Results suggest that the reliability and accuracy of data collected by testing equipment and the enthalpy potential method were reasonable in this study.

3. Effect of faults on performance under cooling model

In this section, we will first explore the effect of a single fault for the VRF system, then expand to double simultaneous faults and triple simultaneous faults. Finally, the trends of some critical features under different faults are analyzed. In the following figures, OC100%, UC 100%, IF 0%, OF 0%, and NC 0 indicate that the VRF system is not faulty.

3.1 Single fault performance effect

Fig.3 shows the impacts of OC faults on the cooling capacity, total system power, COP at four intensities (110%, 120%, 130%, 140%). The right side of the figure is the actual value, and the left side is the ratio of its change to the normal operating conditions. At low OC intensity (less than 110%), the system's cooling capacity decreases less and hardly changes， which was consistent with the results of other studies of TXV-equipped systems[14]. However, when the OC fault is further aggravated, the cooling capacity of the system will drop[8]. Especially when OC intensity is 140%, the system's cooling capacity will drop by 35% compared to normal conditions. At this time, the COP value has increased by 26.14% compared to normal conditions. This abnormal phenomenon is caused when the system’s high voltage reaches the high voltage protection threshold after OC130% intensity. When the refrigerant is overcharged by 130%, a large amount of refrigerant cannot be condensed and accumulates at the end of the condenser, resulting in an abnormal increase in high pressure. At this time, the high voltage protection control will be triggered, e.g. the system compressor frequency reducing. So that the compressor power is reduced[24] and its reduction ratio is greater than the cooling capacity reduction ratio, The former 48.48%, the latter 35.01%. Therefore, there will be a phenomenon that the system COP value is higher than average, but this does not mean that the system performance becomes better. On the other hand, due to the 35.01% reduction in cooling capacity, the system cannot keep the indoor room thermal comfort requirements under the same thermal load.

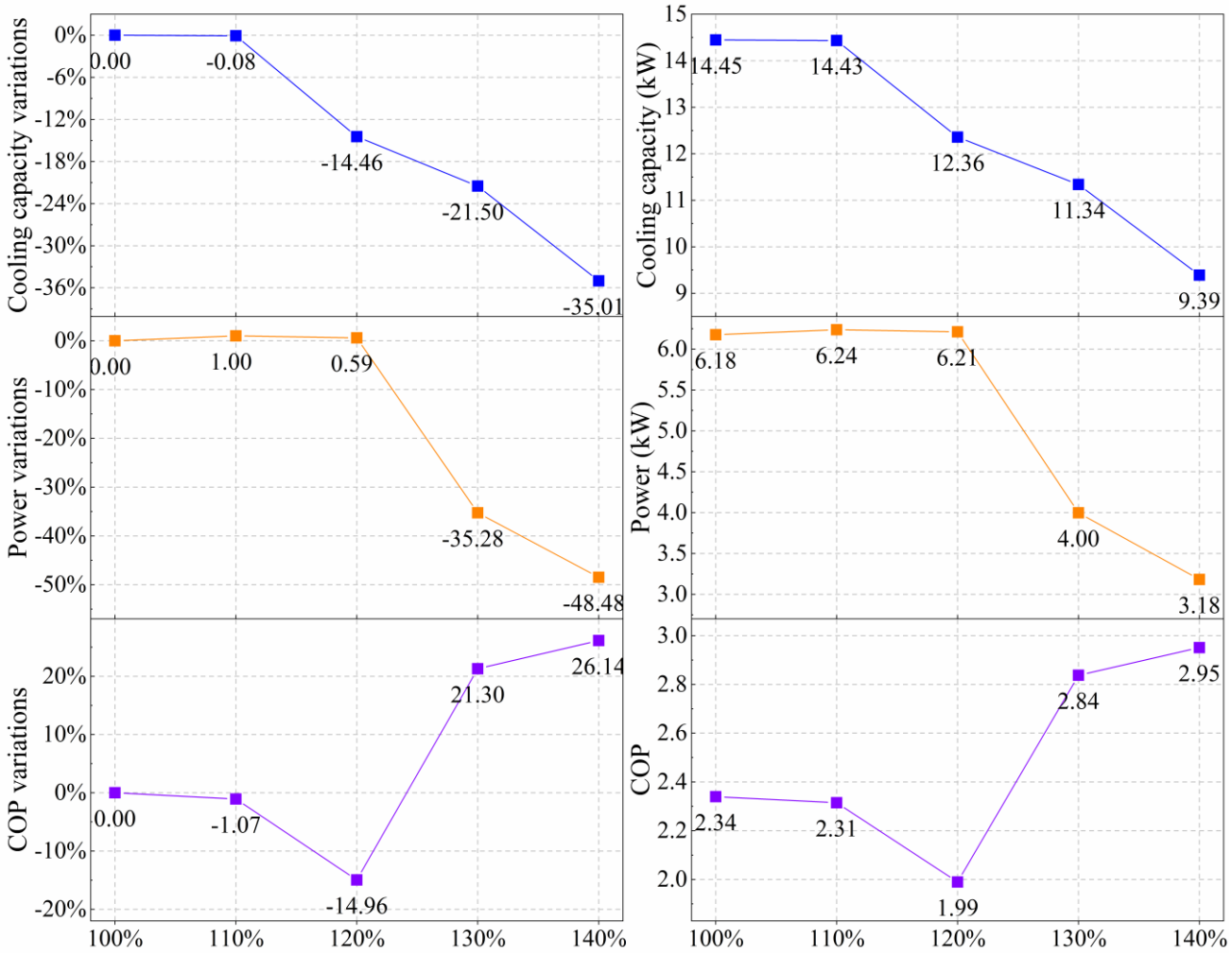

Fig.3 Impacts of refrigeration overcharge faults

Fig.4 shows the impacts of UC faults on the cooling capacity, total system power, COP at five intensities (90%, 80%, 70%, 60%, 50%). The cooling capacity diagram shows that when the fault intensity range is 90%-80%, the system capacity decreases less. This is similar to the discovery by Mehrabi and Yuill[24] at this charge level for the multiple systems they studied. Because in this range of UC fault intensity, the system cooling capacity can maintain a high level by adjusting the opening of the indoor electronic expansion valve (EVI). At this time, the system COP increases to 2.48, an increase of 6.14%. This phenomenon is due to that the compressor needs to reduce the frequency to adjust the high superheat of the system due to the refrigerant undercharge. In contrast, the system's cooling capacity is not attenuated. But this does not mean that refrigerant undercharge is beneficial to the VRF system. The system standard refrigeration charge is the optimal charge volume that meets the system operation under different operation conditions. The UC 90% to 80% fault intensity may not guarantee optimal performance under other working conditions. **Fig.5** shows UC fault impacts under different operating conditions. The horizontal axis represents different fault intensities, and the vertical axis represents the rate of change of each index compared to the normal operation under the same operating condition. From **Fig.5**, it can be found that under 27℃/35℃ operating conditions, the COP values of fault intensity 90% and 80% are reduced by 3.58% and 12.09% respectively compared with

the standard charge. In addition, under the 32℃/43℃ operating condition, the system still obtains more cooling capacity as the fault intensity increases, this is obtained at the cost of additional power consumption. Therefore, its COP value also dropped by 7.84% and 7.45% respectively.

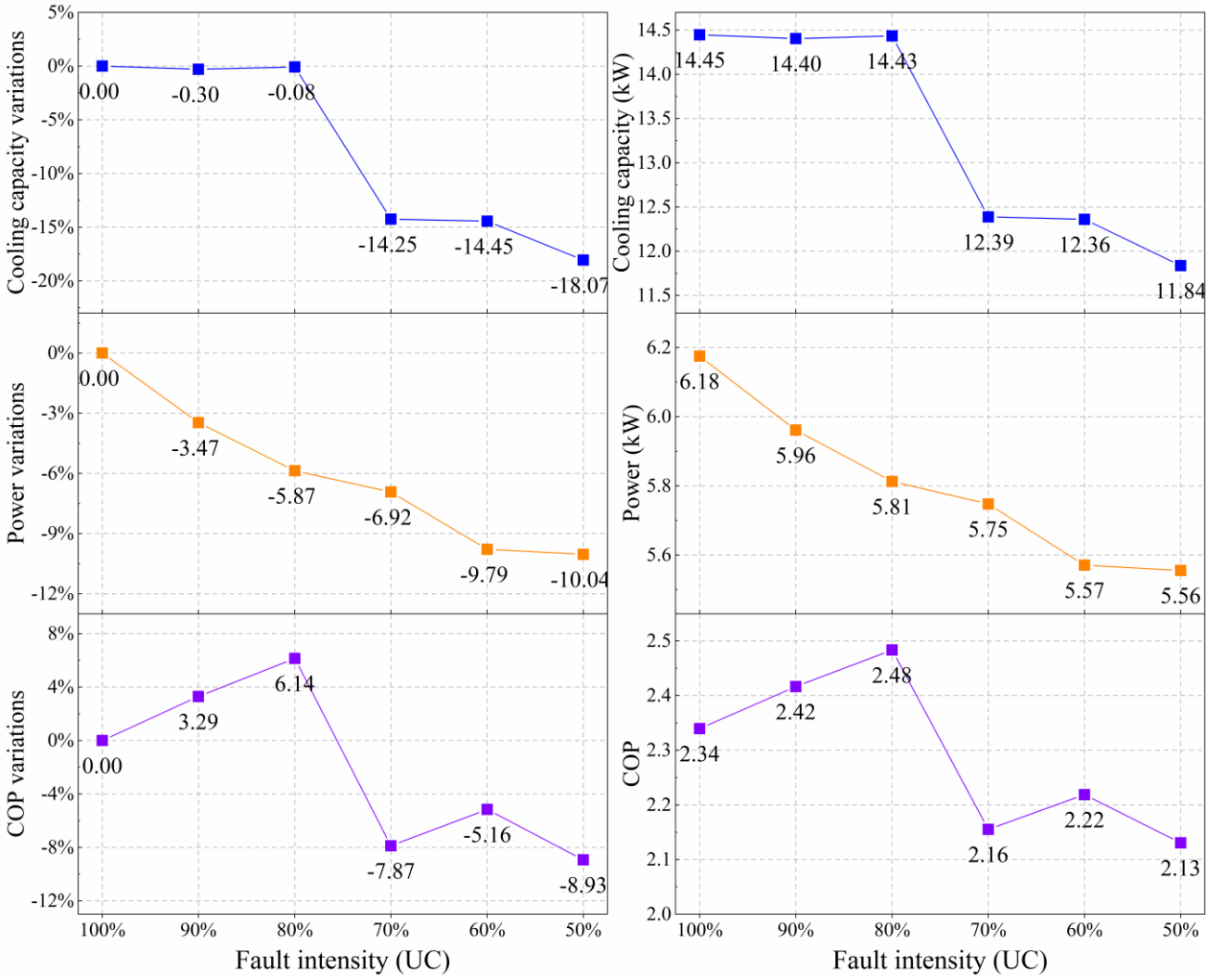

Fig.4 Impacts of refrigeration undercharge faults

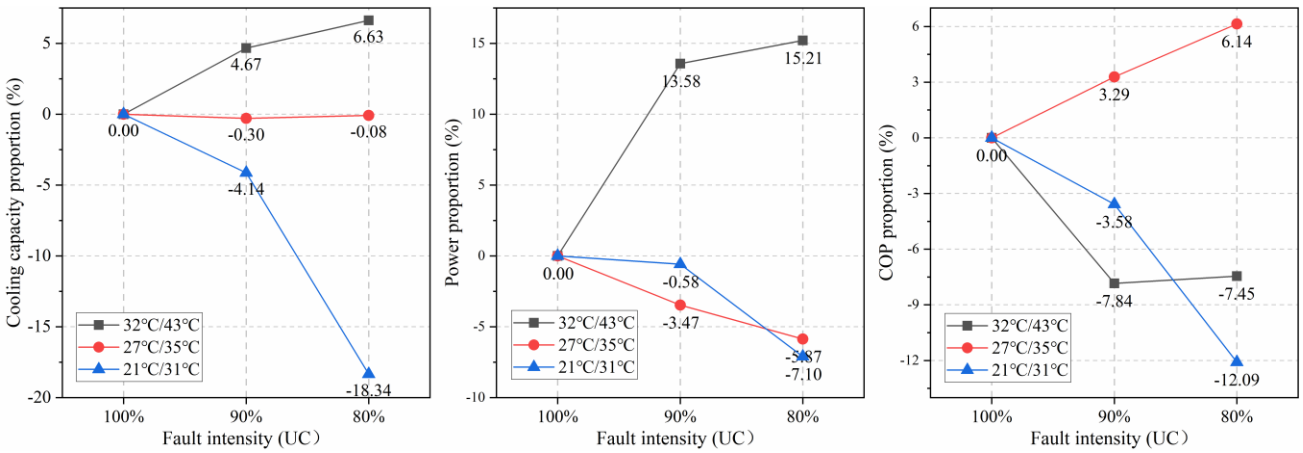

Fig.5 UC fault impacts under different operating conditions (27℃/35℃ means indoor dry bulb temperature 27℃, outdoor dry bulb temperature 35℃)

The cooling capacity and COP of the fault intensity over 70% will drop significantly. The system cooling capacity and COP's reduction ratio in UC 50% fault intensity decrease 18.07% and 8.93%. Compared with the OC and UC fault, it can be found that the refrigeration undercharge fault has a smaller impact on the system than the overcharge fault.

Fig.6 shows the impacts of IF faults on the cooling capacity, total system power, COP at three intensities (25%, 50%, 75%). It can be found that the impact of indoor fouling fault on the cooling capacity gradually increases with the increase of the fault intensity, which was also found by other researchers[8, 15]. In the initial 25% fault intensity increase, i.e. 0% to 25%, the cooling capacity reduction ratio is 8.78%, while in the final 25% fault intensity increase, i.e. 50% to 75%, the cooling capacity reduction ratio is 23.77%. The same fault intensity increase, the cooling capacity reduction rate brought by the difference was 170.73%. The COP indicator also has the same phenomenon. In the early stage of the fault, the impact of each 25% fault intensity is -6.2%, and in the later stage, it can reach -18.09% which is 2.92 times the initial. By contrast, Du et al.[8] found a reduction of about 2% at 22% fault intensity and 4% at 32% fault intensity. This result shows that the later the indoor fouling fault, the greater the impact on the system. In other words, early repair of the indoor fouling fault can effectively avoid the sharp increase impacts on the system in the later stage of the indoor fouling fault. When the system has an IF fault, the phenomenon is similar to the system UC fault; The cooling capacity and system power will be reduced with the fault intensity increase. However, it is evident that the impact of IF fault is more significant than that of UC fault. The former can cause up to 36.84% cooling capacity loss and a 24.38% COP drop in 75% IF fault intensity. At this time, the system can hardly meet the indoor thermal comfort requirements.

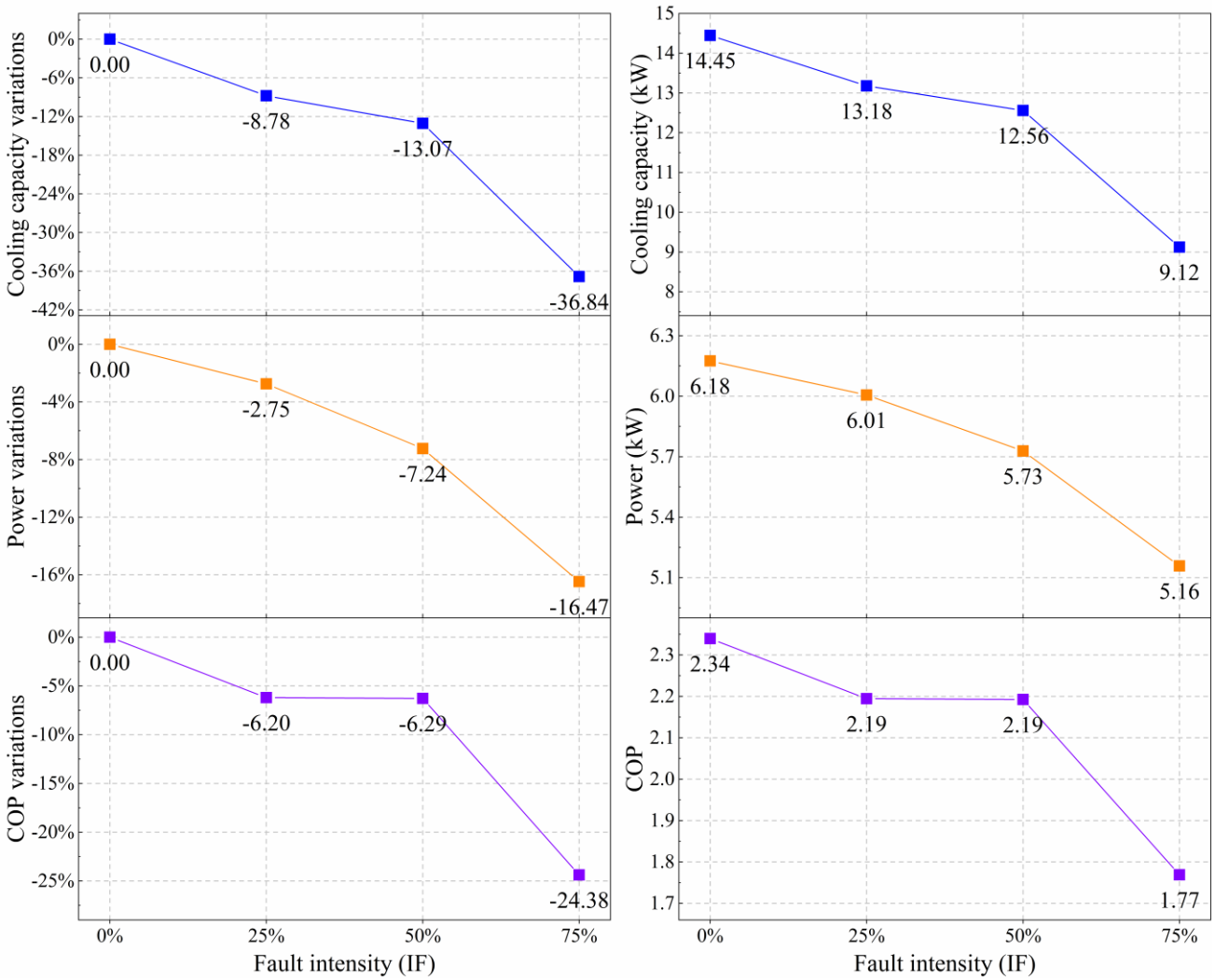

Fig.6 Impacts of indoor units fouling faults

Fig.7 shows the impacts of OF faults on the cooling capacity, total system power, COP at four intensities (25%, 50%, 75%, 100%). The impact of OF fault on the system is more obvious, and it also has the same fault characteristics as IF; That is, as the fault intensity increase, the more significant the impact of the fault. The attenuation of the cooling capacity is similar to the change of the quadratic function, similar to the discovery by Du et al.[8]. When the fault intensity reaches 100%, the cooling capacity drops sharply by 80.27%. At this time, it can be determined that the system has failed. By contrast, according to Du et al.[8] research results, the cooling capacity decays more smoothly and the cooling capacity is reduced by about 7.5% when the OF fault intensity is 35%. It is worth noting that at 50% and 75% fault intensity, the COP value of the system is 6.55% and 11.55% higher than the normal state. But this does not mean that the performance of the system is improved. On the contrary, the VRF system has not guaranteed indoor thermal comfort requirements due to the 26.75% and 46.82% reduction of cooling capacity under the same thermal load. At this time, the system's high pressure is too high due to the OF fault. The compressor frequency is limited, the system's power consumption is greatly reduced and the magnitude is greater than the reduction of the cooling capacity COP value is

increased. Overall, OF fault can cause the cooling capacity to drop by 80.27% and the COP to drop by 47.6%, which is close to complete failure.

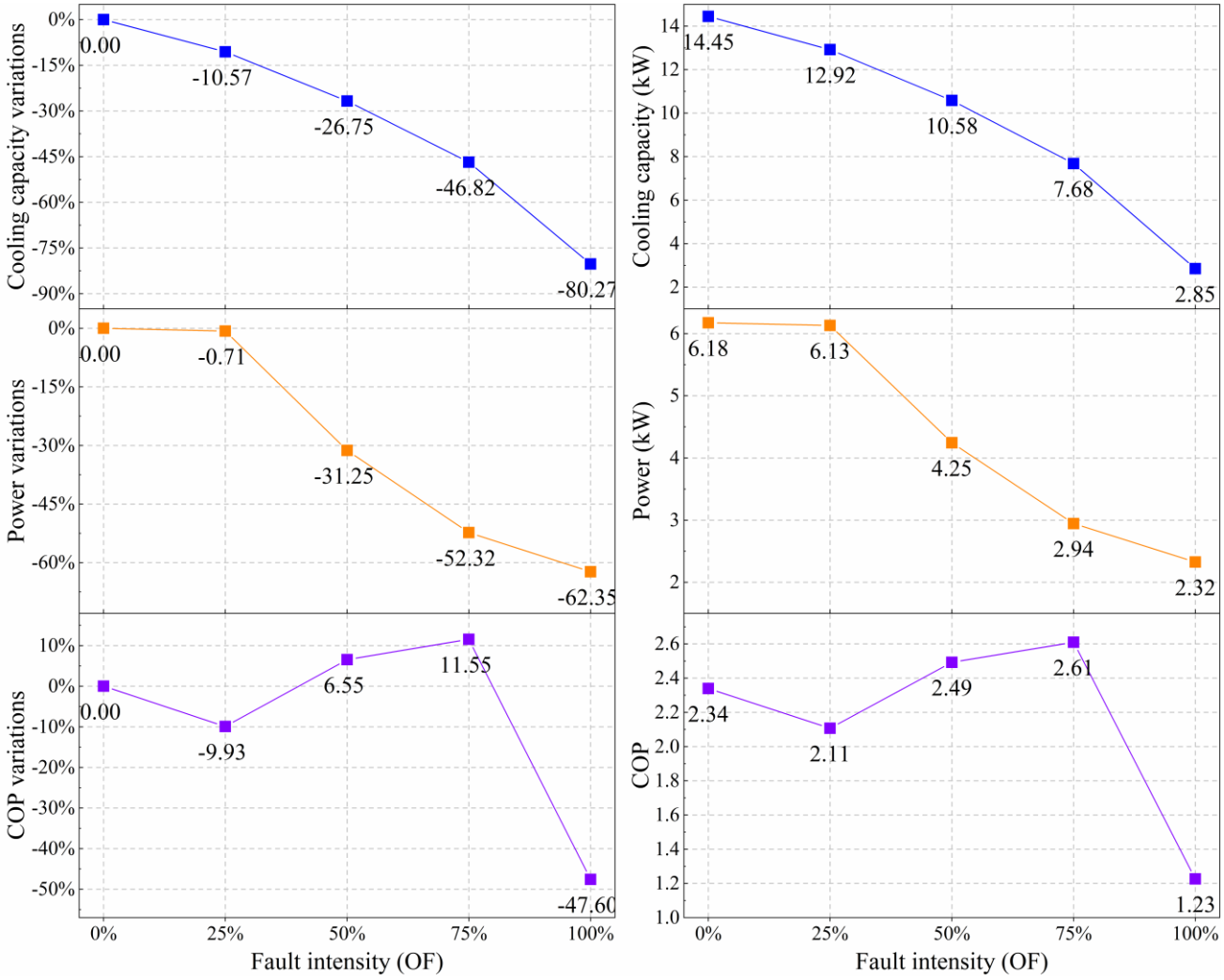

Fig.7 Impacts of outdoor unit fouling faults

Fig.8 shows the impacts of NC faults on the cooling capacity, total system power, COP at three intensities (10g, 20g, 50g). From the perspective of changes in cooling capacity, NC fault has a negligible impact on the VRF system. When the system contains 50g of non-condensable gas, the system's cooling capacity is only reduced by 1.17%. The reduction of COP is only within 3%. This is similar to the discovery by Hu et al.[15], which is decreasing by <1.0% for all operating conditions, and only 1.1%-3.9% with the maximum possible NC fault level. Therefore, it can be concluded that the non-condensable gas has a small impact on the unit's performance in the short term. However, the oxygen in the air will cause the lubricating oil to fail after the long-term operation and cause damage to the compressor. In addition, the mixed oxidation reaction of non-condensable gases may also cause the system to explode. Such hazards can lead to complete system failure, which is highly harmful.

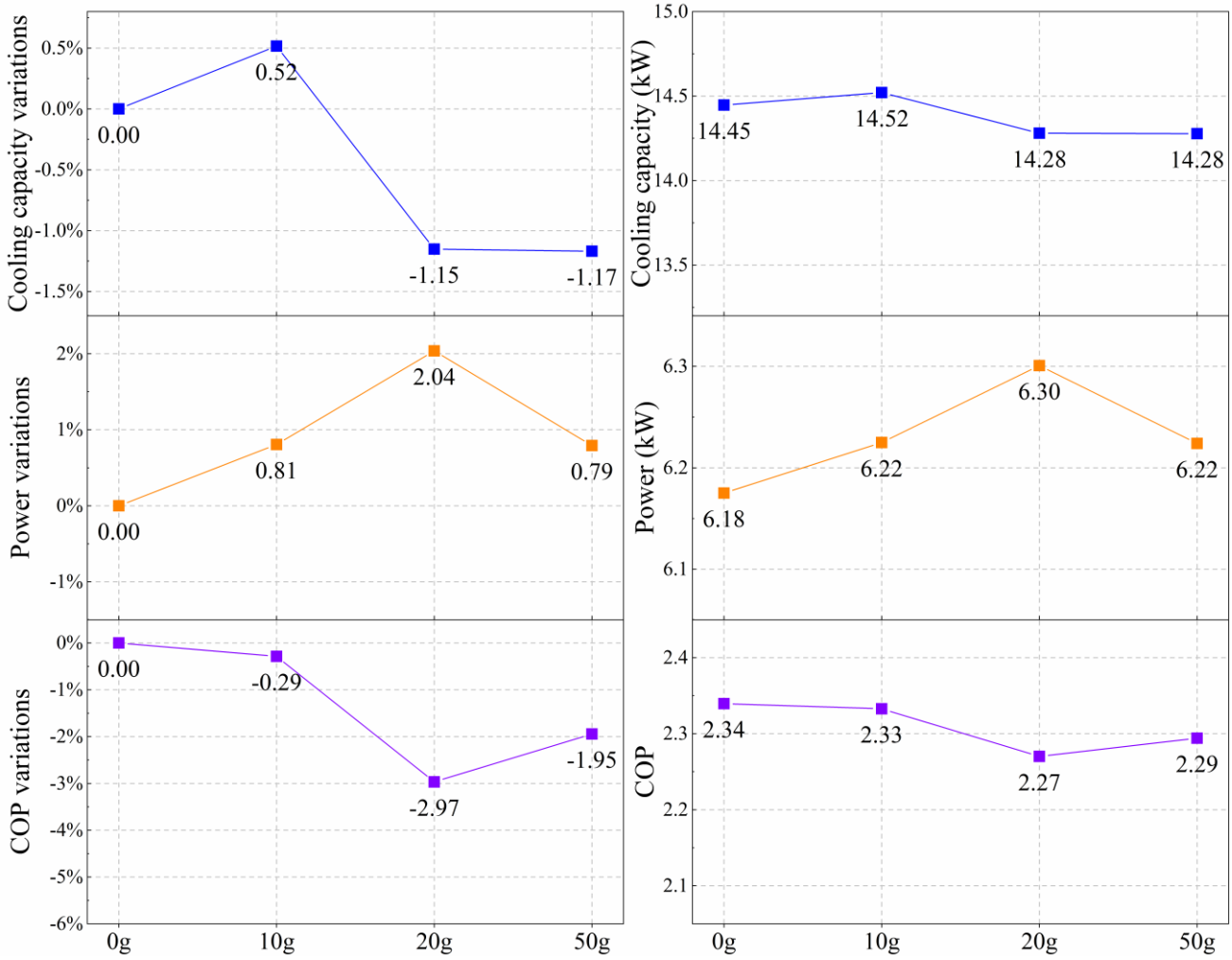

Fig.8 Impacts of non-condensable gas faults

In this section, we analyze the impacts of five common single faults in VRF system. The results show that all five types of faults harm the performance of the VRF system. Among them, the OU fault has the greatest impact, which can cause a 47.6% COP drop and 80.27% cooling capacity reduction. The NC fault that has the least impact on system performance in the short term will reduce the cooling capacity by about 1.1% and the COP value within 3%.

3.2 Double simultaneous fault performance effect

Fig.9 to **Fig.12** show the difference between single-fault and corresponding double simultaneous fault effects on cooling capacity, power, and COP, respectively, to examine the extent to which fault combinations have synergistic or canceling effects.

Fig.9 shows the impacts of "IF+UC/OC" double combination faults. Here, a mixture of IF50 and refrigerant OC120 or UC80 fault is used. First, analyze the simultaneous fault of IF50 and UC80, the results show that the system's cooling capacity will be slightly reduced at this time, but the COP will increase instead, compared to the superimposition of the effects when the two failures occur separately. When the simultaneous fault of IF50 and OC120 occurs, the system performance will not deteriorate compared to the corresponding single fault. Even the COP value has increased by 3.88%. This is

because the IF fault makes the compressor reduce the frequency, offsetting part of the OC120 high load effect, and the simultaneous fault of IF50 and OC120 finally increases the COP value of the system. In general, the simultaneous fault of IF+UC/OC does not make the system performance degradation more serious but can offset each other's adverse effects to a certain extent.

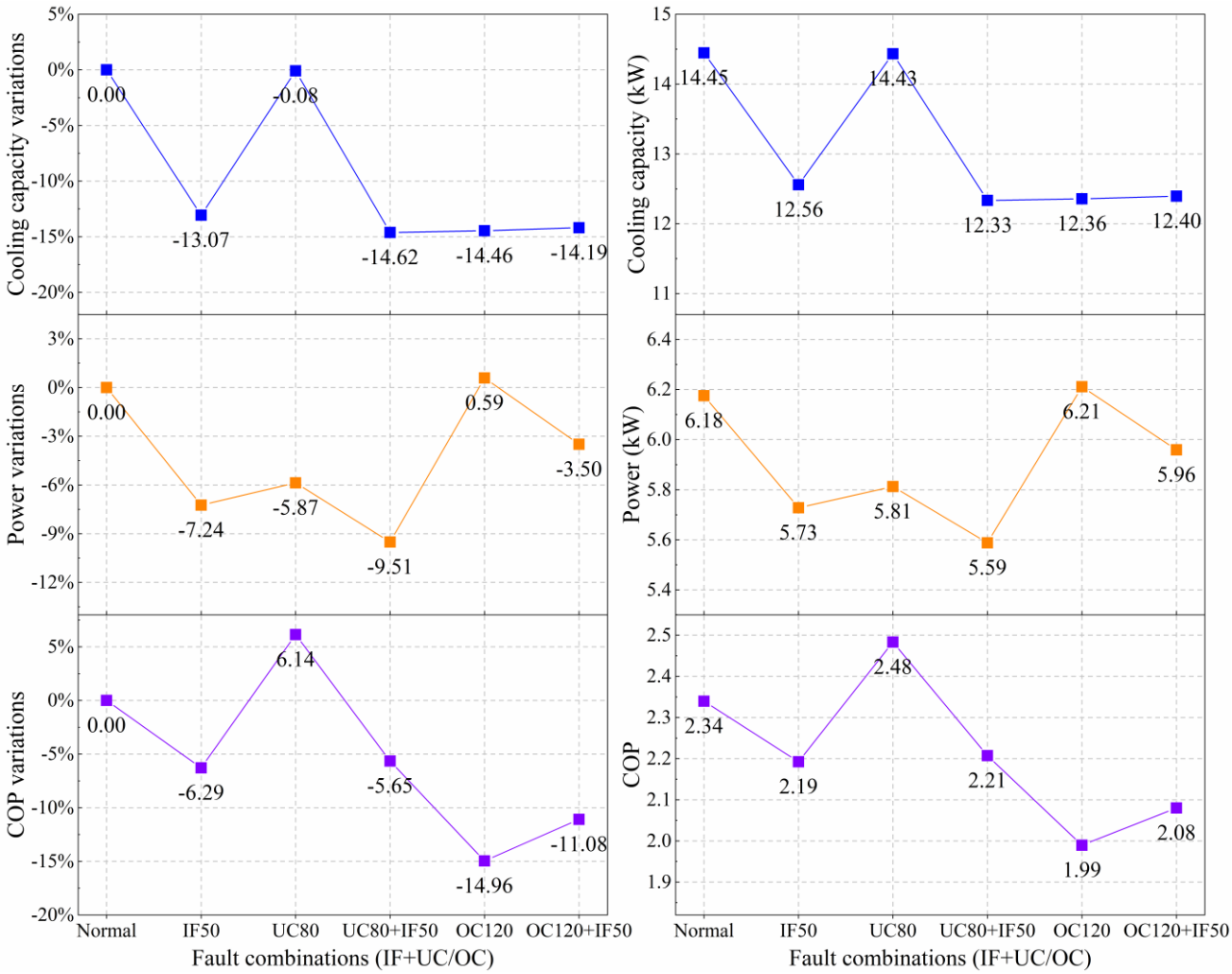

Fig.9 Impacts of double combination faults (IF+UC/OC)

Fig.10 shows the impacts of "IF+OF" double combination faults. From the point of view of the impact on the cooling capacity, these simultaneous faults IF+OF have noticeable superimposing effects. A single OF25 fault impacts -10.57% on the cooling capacity, and the IF50 fault is -13.07%. When these two faults occur simultaneously, the reduction of the system cooling capacity is 22.04%, which is slightly less than the sum of the separate effects of two single faults. It is worth noting that the higher the intensity of OF faults, the superimposed effect of mixed faults will gradually decrease. For example, when only the OF100 fault occurs, the cooling capacity will be reduced by 80.27%, but when it combines with the IF50 fault, the cooling capacity will only be decreased by 83%, only 2.73% more. From the COP chart, it can be found that when IF50+OF50/75 occurs, the system COP value will increase relative to IF50+OF25. This is because the IF50 fault alleviates the huge reduction in the frequency of OF50/75.

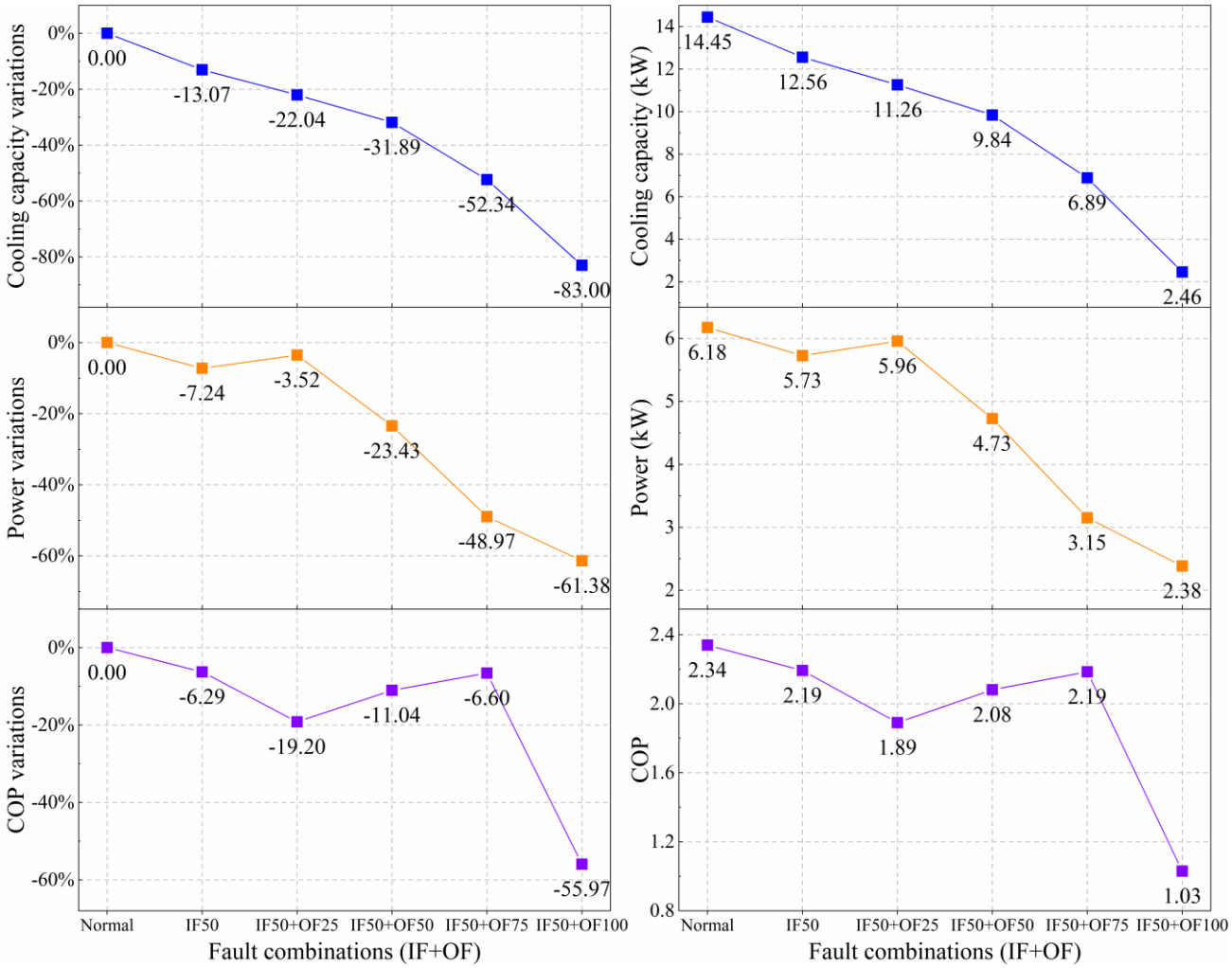

Fig.10 Impacts of double combination faults (IF+OF)

Fig.11 shows the impacts of "OC+OF" double combination faults. Similar to the IF+OF simultaneous faults, the OC+OF simultaneous faults also have obvious superimposing effects. A single OC120 fault impact -14.46% on the cooling capacity, and the OF50 fault is -26.75%. When these two faults occur simultaneously, the reduction of the system cooling capacity is 43.04%, which is 1.83% larger than the sum of the separate effects of two single faults. This result shows that when the system has the simultaneous fault of OC and OF, the system's performance will deteriorate more severely. However, the superposition of this influence has a certain limit. When OF fault intensity is increased from 50% to 75%, the cooling capacity attenuation of the simultaneous fault OC120+OF75 is 45.71%, which is only an increase of 2.67% compared with OC120+OF75 simultaneous fault. This result shows that when the fault intensity of one single fault is further increased, its superimposing effect will not increase drastically. From the single fault analysis, we know that when the system has an OF fault, the COP value of the system will increase due to the greatly reduced frequency of the compressor. This phenomenon becomes more obvious after the overcharge fault is simultaneous. In this case, the power of the system decays to half of the normal value.

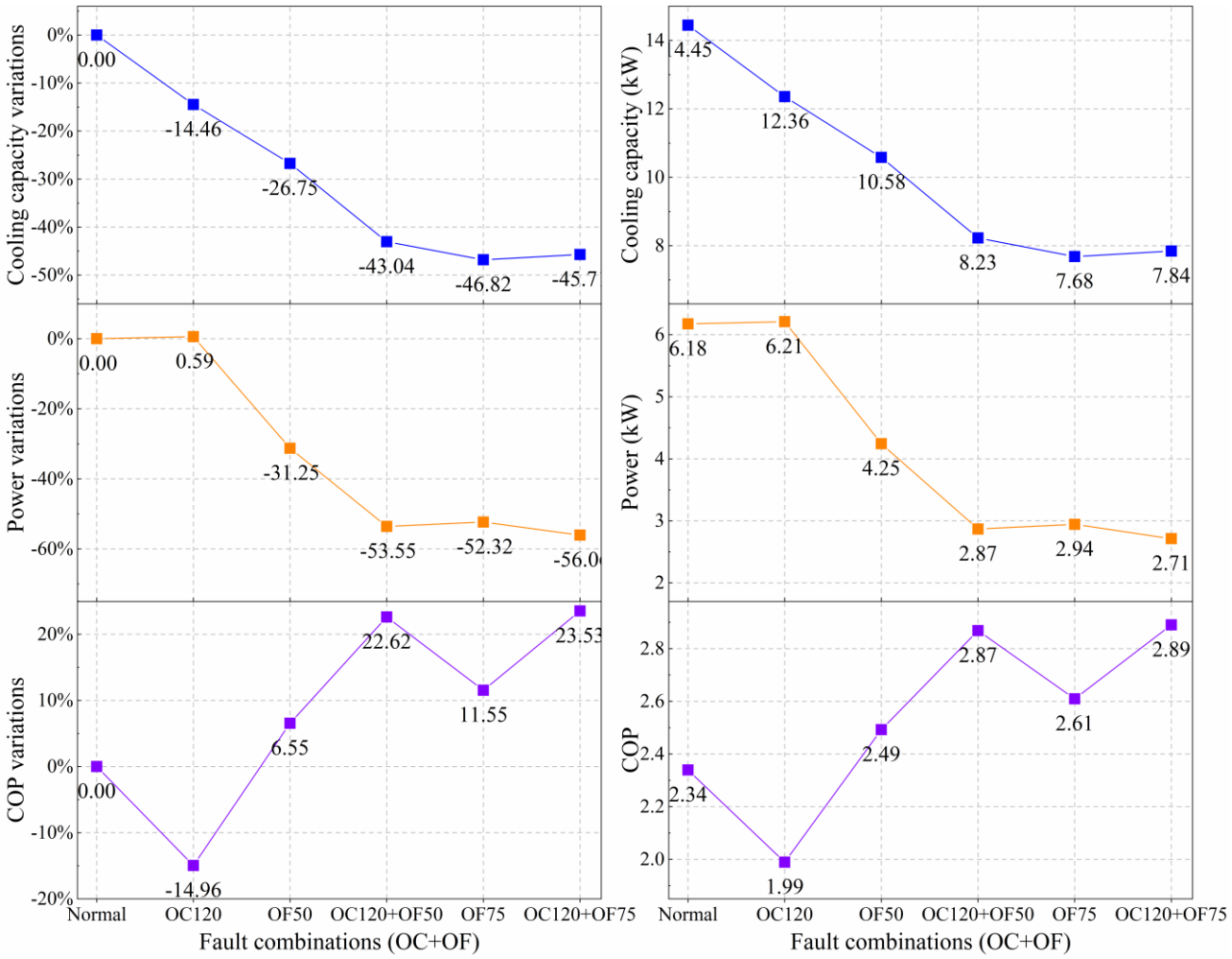

Fig.11 Impacts of double combination faults (OC+OF)

Fig.12 shows the impacts of "UC+OF" double combination faults. From the perspective of system cooling capacity, when the system occurs UC80+OF50 simultaneous fault, the cooling capacity attenuation is 17.54%. However, even a single OF50 fault has an impact of -26.75% on the cooling capacity. This phenomenon shows that the simultaneous fault of UC+OF has canceling effects for VRF system performance. However, these canceling effects will weaken as the fault intensity increases. For example, when the OF fault intensity is increased from 50% to 75%, the cooling capacity attenuation of the simultaneous fault UC80+OF75 is 45.3%, which is only 1.6% less than the combined value of two single faults. This also shows that there will be different performance effects on the results in the double simultaneous fault of different fault intensities. This mixture of faults, which have the canceling effects for VRF system performance, makes the law of VRF system performance changes more complicated.

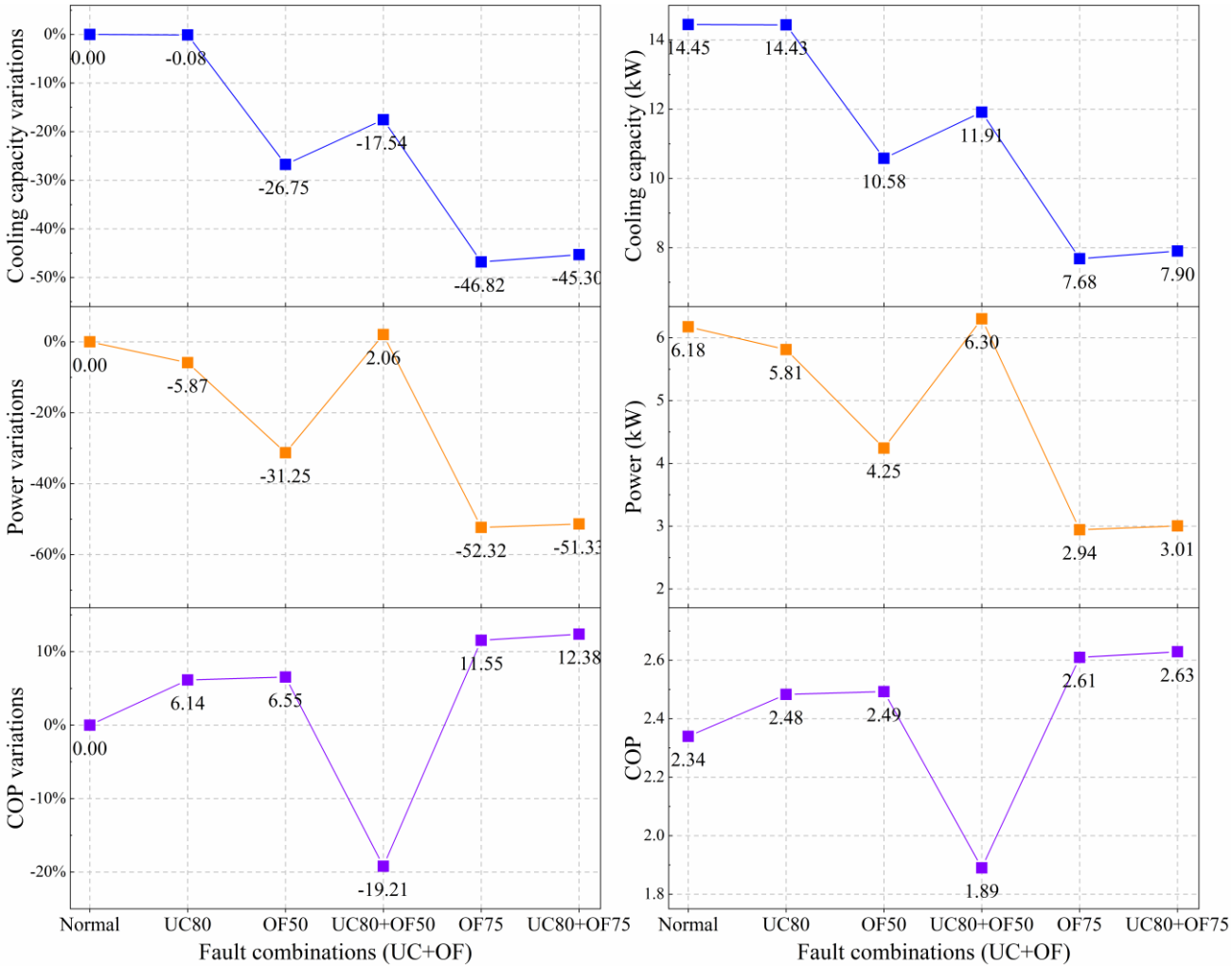

Fig.12 Impacts of double combination faults (UC+OF)

In general, the impact of double simultaneous faults on system performance presents two characteristics. First canceling effect, that is, if two faults occur simultaneously, the impact of the fault on the system performance will cancel each other out. The typical simultaneous fault with canceling effect is UC+OF. The canceling effect on the system cooling capacity can reach 9.21%. Second superimposing effect, that is, if two faults occur simultaneously, the impact of the fault on the system performance will superimpose each other out. The typical simultaneous fault with superimposing effect is OC+OF. It is worth noting that this superimposing effect is more obvious at low fault intensity.

3.3 Triple simultaneous fault performance effect

Adopt the same method of analyzing double faults; in this section we present results for triple simultaneous faults. **Fig.13** and **Fig.14** present the impacts of cooling capacity, power, and COP for three simultaneous faults. Except for the normal condition, all other triple-fault combinations also compared to corresponding double simultaneous.

Fig.13 shows the impacts of "OC120+IF50+OF50/75" three simultaneous faults. The impact of these three single faults (OC120, IF50, OF50) on the cooling capacity are -14.46%, -13.07%, and -26.75% in sequence. The impacts of corresponding double faults (OC120+IF50, OC120+OF50,

IF50+OF50) are -14.19%, -43.04%, and -31.89%. From **Fig.13** we know that the OC120+IF50+OF50 simultaneous fault of these three faults impacts the system's cooling capacity by -44.51%, which is 9.77% less than the combined value of three single faults. And it is only 1.47% greater than the impact of the OC120+OF50 simultaneous fault. This result shows that in the three-fault mixture, IF50 fault can still compensate for the negative effects of these faults. This result is also true in the OC120+IF50+OF75simultaneous fault. In addition, in triple simultaneous fault, the deterioration of one of the fault intensities will also aggravate the overall impact of the cooling capacity. For example, in the OC+IF+OF simultaneous faults, the OF fault intensity changes from 50% to 75%, and the system cooling capacity attenuation changes from 44.51% to 50.71%. In addition, we can see that when the OC+IF+OF simultaneous faults occur, the COP of the system increases sharply. This is also due to the superimposed effect of OF fault. This also shows that under simultaneous fault, faults will affect each other.

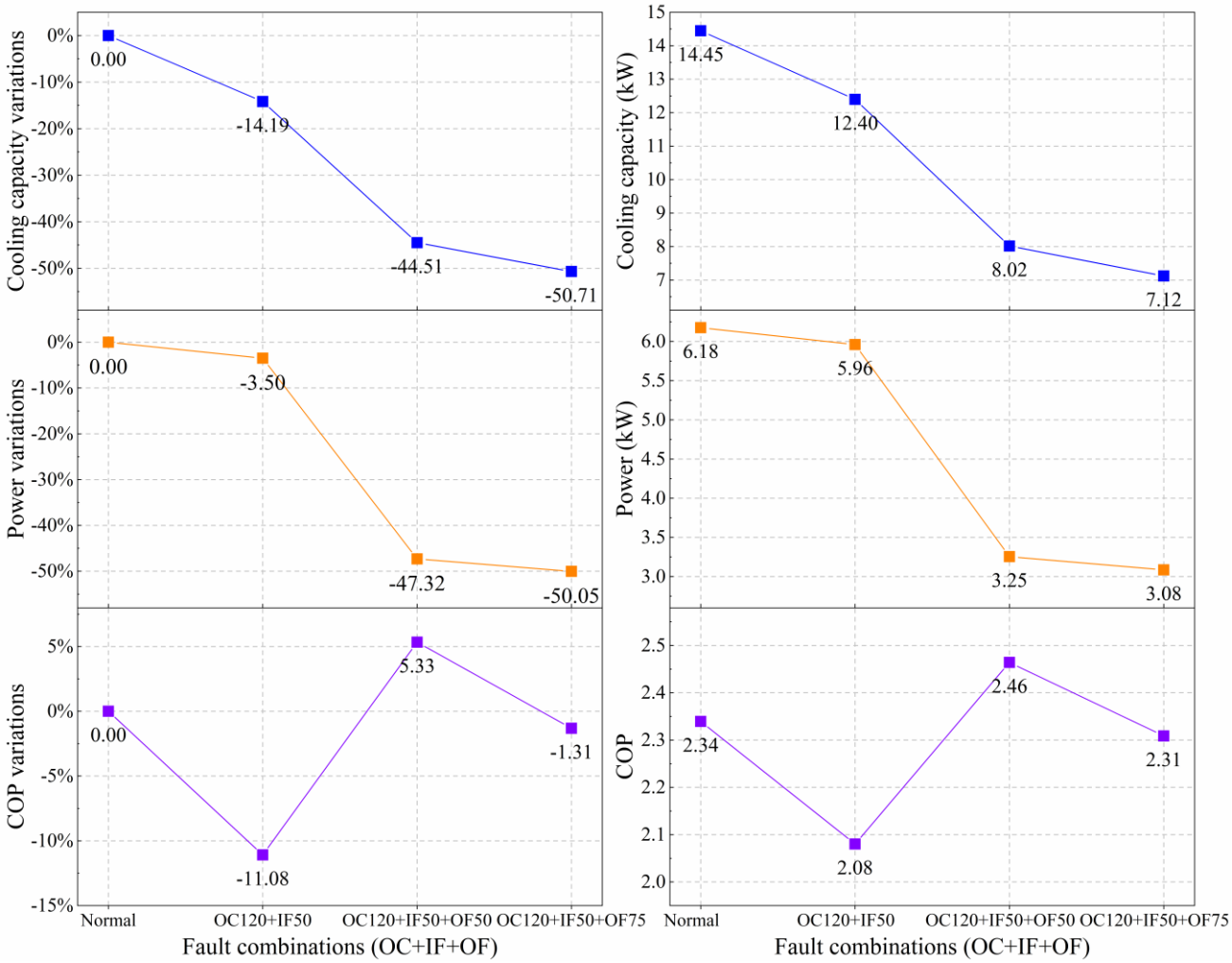

Fig.13 Impacts of triple combination faults (OC+IF+OF)

Fig.14 shows the impacts of "UC120+IF50+OF50/75" three simultaneous faults. Interestingly, although UC80, imposed individually, had no significant effect on cooling capacity, when it is combined with other faults, it can compensate for the negative effects of these faults. The impact of these three single faults (UC80, IF50, OF50) on the cooling capacity are -0.08%, -13.07%, and -26.75%

in sequence. The impacts of corresponding double faults (UC80+IF50, UC80+OF50, IF50+OF50) are -14.62%, -17.54%, and -31.89%. When three faults co-occur, the UC80 fault can reduce the -31.89% impact of the original IF50+OF50 fault to -26.75%. This is mainly due to that the undercharge fault can effectively avoid the system high-pressure frequency limitation problem caused by outdoor fouling. This impact is still effective when one of fault intensity is increased. For example, when the OF fault intensity is increased from 50% to 75% in UC+IF+OF simultaneous faults, the UC80 fault can still reduce the original 52.34% adverse impact of IF50+OF75 to 46.78%. We see that the attenuation rate has changed by 5.56%, which is basically the same as the 5.14% change in the case of UC80+IF50+OF50 fault circumstances. This shows that the compensation of the negative effects of UC80 will not change significantly because of one of fault intensity increases.

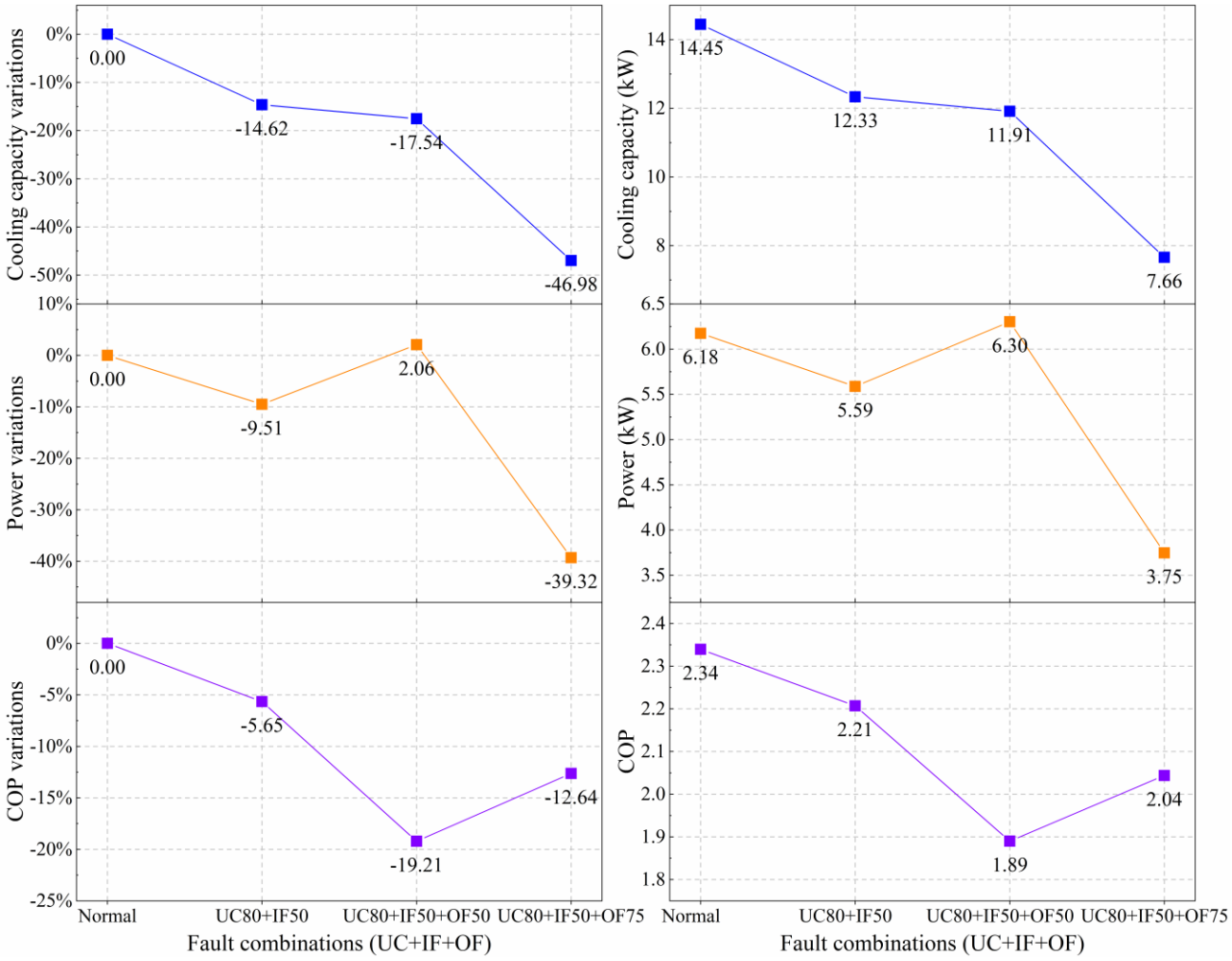

Fig.14 Impacts of triple combination faults (UC+IF+OF)

3.4 Trend analysis

System variables are measurable performance indicators, and they play an excellent role in understanding system conditions. Understanding the trend of system variables under fault conditions forms the basis of the field of fault detection and diagnosis. To find the magnitude of the feature deviation from normal condition, we define feature variations, defined in **Eq. (11)**.

$$Variation_{feature\_i} = \frac{feature\_i_{fault} - feature\_i_{normal}}{feature\_i_{normal}} \quad (11)$$

where $feature\_i_{fault}$ and $feature\_i_{normal}$ are the measured values of feature *i* from the faulted condition and normal condition, respectively.

We selected six important variables (shown in **Table 4**) to analyze the influence trend of the fault on these characteristic variables. In addition, the changes in magnitude are also useful for some data-driven-based FDD methods to classify the fault type. To facilitate comparison and analysis, the trend impacts of a different single fault, simultaneous faults, and their different fault intensities on a certain variable is plotted in a chart.

Table 4 Definitions of selected six features

Symbol	Definition	Uint
P_d	Compressor discharge pressure	Mpa
P_s	Compressor suction pressure	Mpa
$T_{\_suc}$	Compressor suction temperature	℃
$T_{\_dis}$	Compressor discharge temperature	℃
$T_{\_sc}$	Condenser supercooling temperature	℃
$T_{\_sh}$	Discharge superheat temperature	℃

Fig.15 presents the trend impacts of P_d feature in different types of fault. OC fault and UC fault will lead to opposite P_d trends, and its variation trend has a clear positive correlation with the fault intensity. The former will cause the P_d feature larger, and the latter will cause the P_d feature to become smaller. Through **Fig.15**, we can find that IF and UC's trend impacts for Pd feature are similar, and the OF and OC are identical. The non-condensable gas cannot be condensed in the condenser and accumulates, making P_d feature higher. However, from a quantitative point of view, its impact is far less than the high fault intensity OC, UC, IF, OF faults. This is consistent with the conclusion that NC fault has little impact on system performance in Section 3.1. In simultaneous faults, a significant finding is that the upward trend of P_d feature is a dominant characteristic. When faults occur simultaneously, as long as one fault can cause P_d feature to become higher, the final simultaneous faults result is that the system pressure becomes higher. Only when the two faults both lead to a reduction in P_d feature, the system P_d value will decrease, and of course the two will have a certain promotion effect. As shown in **Fig.15**, the P_d value in the simultaneous fault result shows a negative trend only when the two faults of UC and IF co-occur. And we can find that the P_d variation of UC80 is 6.23%, and the IF50 is 4.89%, but the simultaneous fault UC80+IF50 is 7.92%. This phenomenon shows that these two faults have mutually promoting effects.

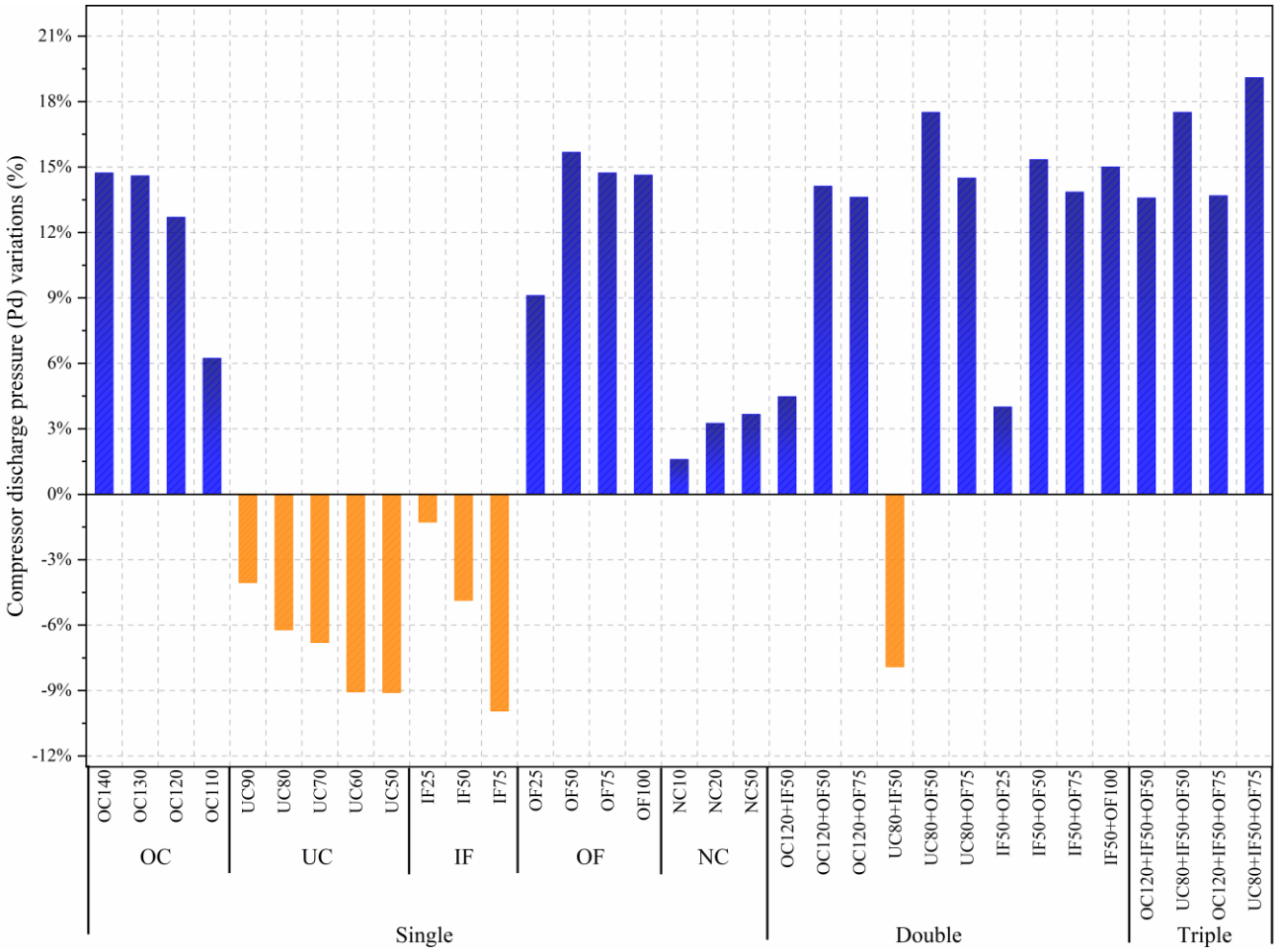

Fig.15 compressor discharge pressure (P_d) variations in different fault type and fault combination

Fig.16 presents the trend impacts of P_s feature in different types of faults. It can be seen from **Fig.16** that most of the faults cause the system P_s feature to increase and only the UC and IF faults will cause it to decrease. And only the UC fault intensity is high, the P_s feature will reduce. This shows that when the UC fault intensity is low, the system can keep the P_s feature in a normal range by adjusting the compressor frequency and valve opening. When OF fault intensity is over 25%, P_s feature will increase significantly, and as the fault intensity increases, the variation range will be greater. The maximum variation is 108.52%, which is 15.2 times the absolute value of maximum UC P_s feature variation, 14.1 times that of NC fault, 3.6 times that of IF fault, and 2.2 times that of OC fault. This is because when the outdoor heat exchanger has poor heat dissipation, the condensing temperature rises and then causes the evaporation temperature to rise. The low pressure of the system becomes higher. This effect continued in double simultaneous faults containing OF fault. For example, fault of OC120+OF50/75, UC80+OF75, IF50+OF50, etc., caused the Ps feature to rise by more than 60%. Interestingly, when the three types of faults UC/OC, IF, and OF fault occur simultaneously, the rising trend of the system P_s feature is suppressed. From the results, the maximum P_s variation is 40%. This shows that IF50 fault has a strong effect of offsetting the upward trend of other faults. This phenomenon was also verified in double simultaneous fault OC120+IF50 and IF50+OF25. Initially, UC120 and OF25 have 6.25% and 7.53% P_S variation effects, but when it occurs simultaneously with IF50, the corresponding simultaneous fault Ps variations are -13.49% and -7.67%. IF50 can change the original positive trend into a negative trend.

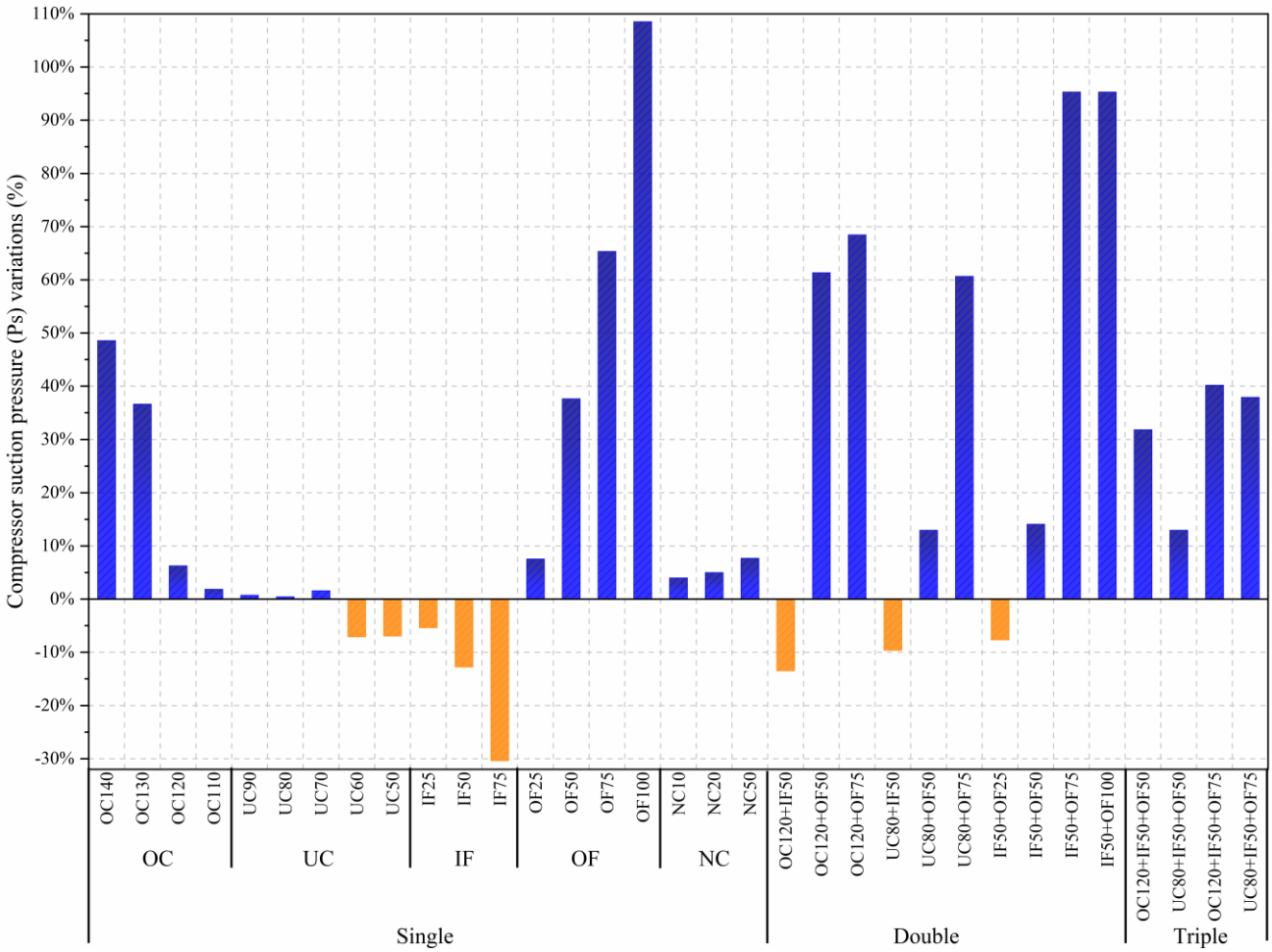

Fig.16 Compressor suction pressure (P_s) variations in different fault type and fault combination

Fig.17 presents the trend impacts of $T_{\_suc}$ feature in different types of faults. $T_{\_suc}$ feature will only show a downward trend when the IF fault occurs, and the proportion of decline increases sharply with the intensity of the fault, and finally reaches -721.43%. When the IF fault occurs, the refrigerant cannot evaporate effectively, causing a large amount of liquid refrigerant to accumulate in the indoor units. At this time, the pressure drop in the evaporator increases, resulting in a decrease in suction temperature. The greater the intensity of IF fault, the more serious the indoor units' liquid floodback, and the greater the drop in suction temperature. Therefore, it can be considered that $T_{\_suc}$ feature can be used as a characteristic variable for identifying OF fault. Correspondingly, the OF fault makes $T_{\_suc}$ feature has a significant increasing trend. When OF fault intensity is 100%, $T_{\_suc}$ feature has the largest variation, reaching 1578.57%. In terms of magnitude, NC fault has the least impact on the $T_{\_suc}$ feature. Similar the Ps feature, the IF fault has a strong offsetting effect, so that the increasing trend of the $T_{\_suc}$ feature is alleviated. Even in minor fault intensities, the original positive trend becomes a negative trend, e.g., OC120+IF50, UC80+IF50, and OF25+IF50.

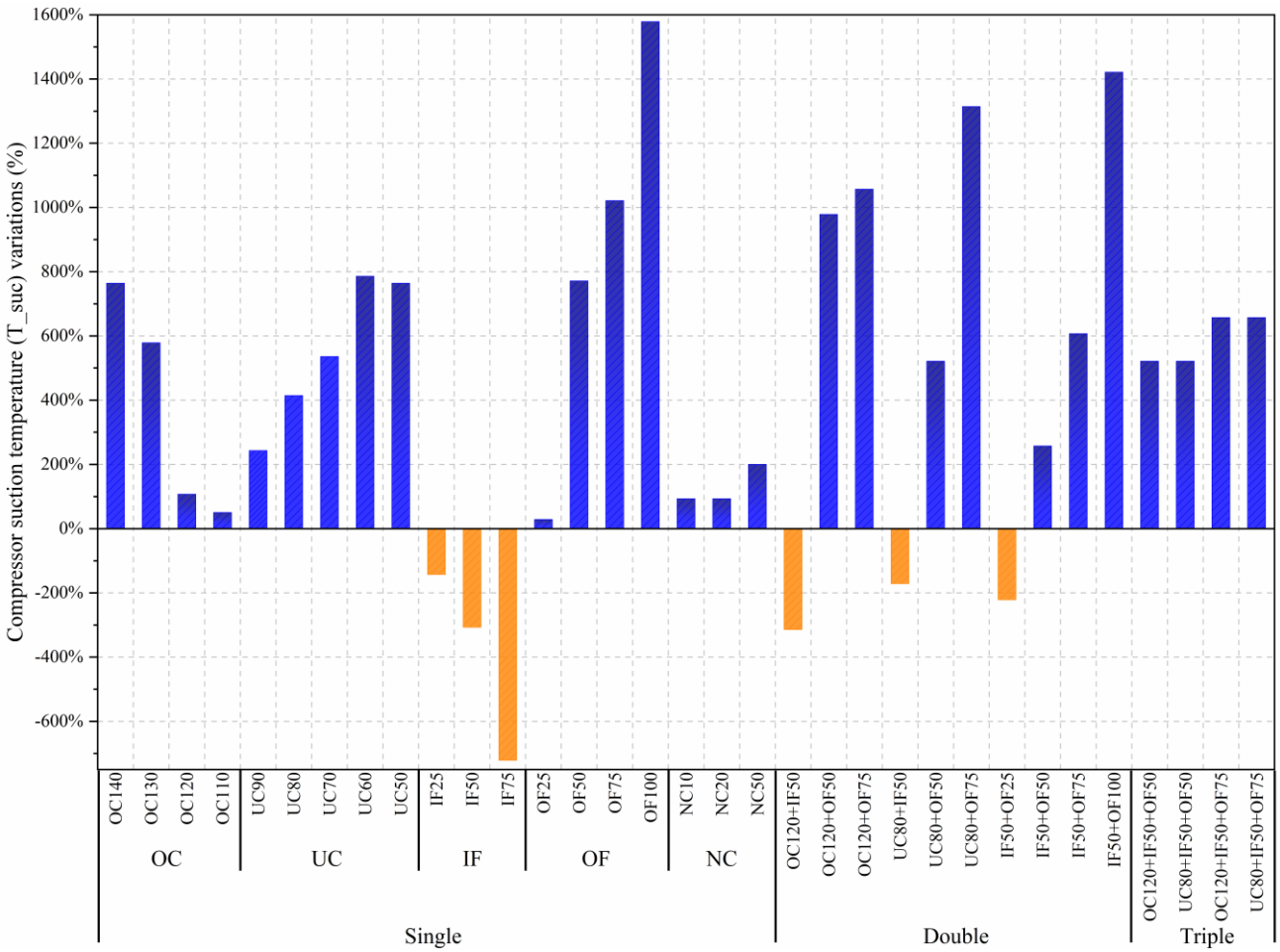

Fig.17 Compressor suction temperature (T_{suc}) variations in different fault type and fault combination

Fig.18 presents the trend impacts of T_{dis} feature in different types of faults. Intuitively, the trend of T_{dis} feature caused by other faults is much more complicated. For example, OF fault, when the fault intensity is lower, the T_{dis} feature shows a positive trend, and as the fault intensity increases, the greater the variation. However, when the fault intensity is large to a certain extent (e.g.75%), the T_{dis} feature will show an opposite trend. With the increase of the fault intensity, the greater the variation. IF faults are more complicated. When the fault intensity is 25%, the variation of T_{dis} feature is -1.83%, and when the fault intensity becomes 50%, there is almost no change. Still, when the fault intensity rises to 75%, it causes -1.70% variation. As a result, the trend of the T_{dis} feature in simultaneous faults is also complex and diverse. The T_{dis} feature variations of OC120 and OF50 were 3.53% and 9.29% in corresponding single fault, respectively. However, in the OC120+OF50 simultaneous fault, its variation has become -8.64%. By consulting the unit control results, it was found that when the two faults co-occurred, the compressor entered the high-pressure protection control, which reduced the frequency and caused the discharge temperature to decrease. This also explains why the T_{dis} feature increases when UC80+OF50 and UC80+OF75 fault occur. It's because the refrigeration undercharge makes the compressor frequency up.

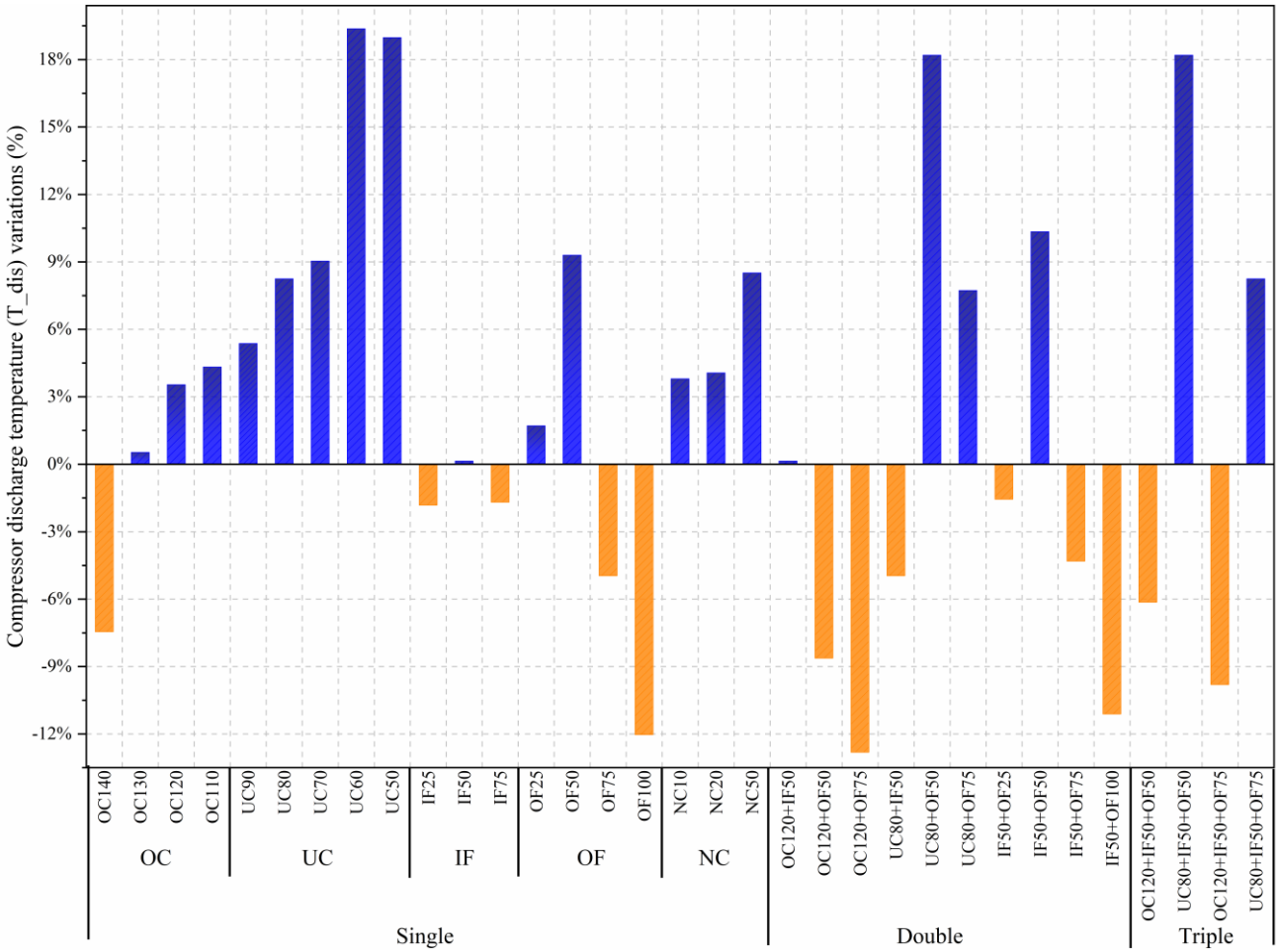

Fig.18 Compressor discharge temperature ($T_{\_dis}$) variations in different fault type and fault combination

Fig.19 presents the trend impacts of $T_{\_sc}$ feature in different types of fault. The $T_{\_sc}$ feature can be used to distinguish OC and UC faults very well. When OC fault occurs, the trend of $T_{\_sc}$ feature is positive, bigger than 40%. While the trend is negative when UC fault occurs. This is because when the system refrigeration is undercharged, the relative area of the condenser increases and the corresponding saturation temperature decreases, resulting in a decrease in the $T_{\_sc}$ feature.

Conversely, when the system refrigeration is overcharged, the condensing pressure rises, and the corresponding saturated condensing temperature also rises. However, because the excess refrigerant accumulates at the bottom of the condenser and exchanges heat with the environment sufficiently, the outlet temperature of the condenser is close to the ambient temperature, which causes the $T_{\_sc}$ feature increasing. When the IF fault intensity is large, it will also cause a negative trend variation in the $T_{\_sc}$ feature. But its impact is far less than UC fault. It is worth noting that when the OF fault intensity is lower, the $T_{\_sc}$ feature increases, but when the fault intensity reaches 100%, there will be a great negative trend variation. This is caused by poor heat dissipation of the outdoor unit. When the OF fault intensity is very high, the refrigerant cannot be condensed and is directly output in the form of high-temperature gas, and the $T_{\_sc}$ feature is drastically reduced. The simultaneous fault analysis shows that the negative trend of $T_{\_sc}$ feature caused by UC and IF fault is a weak influence, liking a recessive. Because only when these two faults co-occur, the simultaneous faults will eventually show a negative

trend. Once other faults can lead to a positive trend variation, the simultaneous faults must eventually show a positive trend variation.

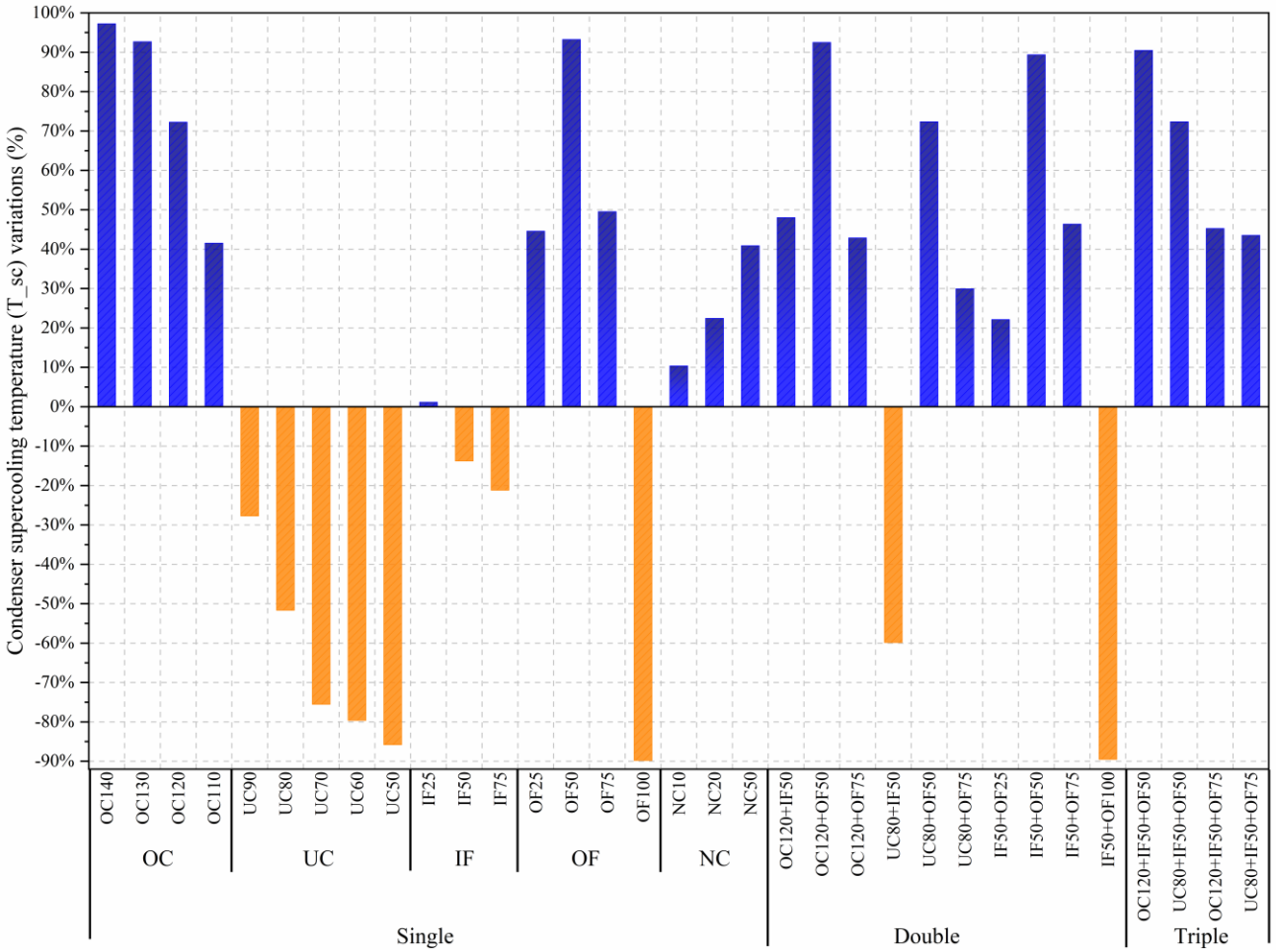

Fig.19 Condenser supercooling temperature (T_{sc}) variations in different fault type and fault combination

Fig.20 present the trend impacts of T_{sh} feature in different types of faults. The T_{sh} feature has an apparent negative correlation with the refrigerant charge. The larger the refrigerant amount, the smaller the T_{sh} feature. Because if the performance of the compressor remains unchanged, the discharge temperature will be relatively unchanged. The condenser's saturation temperature will increase when refrigerant increases, decreasing the T_{sh} feature. The impact of OF and IF fault on the T_{sh} feature is much more complicated. The variation may show the opposite trend with the different intensities of fault. In OF faults, when the fault intensity is low, its impact on the T_{sh} feature is negative, with a value of 9.17%. However, when the fault intensity is increased to 50%, the impact becomes a positive trend with a value of 3.55%.

What's more varied is that when the fault intensity increases, the trend becomes negative again, and as the fault intensity increases, the greater the negative trend value. The OF100 fault has the most serious impact on T_{sh} feature, which can reach -56.74%. The negative trend of T_{sh} feature caused by OC fault is a dominant characteristic. This means that as long as the OF fault is included, the simultaneous faults must cause a negative trend variation to the T_{sh} feature.

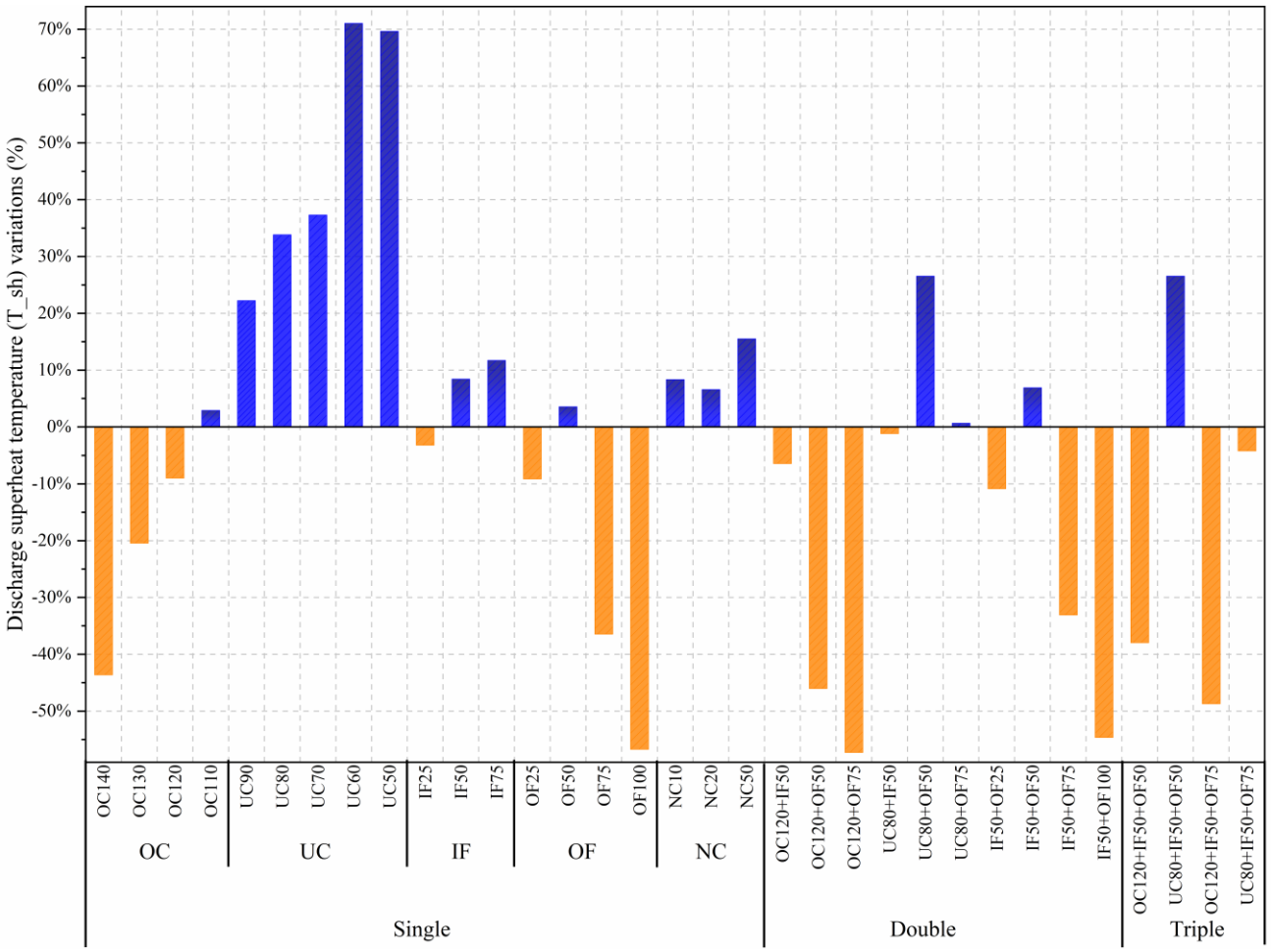

Fig.20 Discharge superheat temperature (T_{sh}) variations in different fault type and fault combination

In the end, according to the analysis of the results in **Fig.15** to **Fig.20**, the trend of six typical variables in different single faults or simultaneous faults can be concluded as shown in **Table 5**. In the table, "↑" indicates a positive trend, also called an upward trend and the corresponding "↓" indicates a negative trend, also called a downward trend. It is worth noting that " Uncertain " means that the changing trend is not clear; the variation trend will have an opposite trend as the fault level increases.

Table 5 Six variables trends in different fault situation summary

Numb	Types	P_d	P_s	T_{dis}	T_{suc}	T_{sc}	T_{sh}
1	OC	↑	↑	Uncertain	↑	↑	↓
2	UC	↓	Uncertain	↑	↑	↓	↑
3	IF	↓	↓	Uncertain	↓	↓	Uncertain
4	OF	↑	↑	Uncertain	↑	Uncertain	Uncertain
5	NC	↑	↑	↑	↑	↑	↑
6	OC+IF	Uncertain	Uncertain	Uncertain	Uncertain	↑	Uncertain
7	OC+OF	↑	↑	↓	↑	Uncertain	↓

8	UC+IF	↓	↓	Uncertain	Uncertain	↓	↑
9	UC+OF	↑	↑	↑	↑	Uncertain	Uncertain
10	IF+OF	↑	Uncertain	Uncertain	Uncertain	Uncertain	Uncertain
11	OC+IF+OF	↑	↑	↓	↑	Uncertain	↓
12	UC+IF+OF	↑	↑	↑	↑	Uncertain	Uncertain

4. Conclusions

This paper demonstrates an extensive experimental effort dedicated to solving critical problems related to VRF systems' fault detection. Different fault intensities, fault types and simultaneous faults such as double simultaneous and triple simultaneous are all considered. The cooling capacity, system power, and COP are used as indicators of performance impact. In addition, the impacts caused by different faults on system parameter variables are also be analyzed and summarized. Several core conclusions were listed below：

(1) The results show that all five types of faults harm the VRF system's performance. Among them, the outdoor fouling fault has the most significant impact, which can cause a 47.6% COP drop and 80.27% cooling capacity reduction at 100% fault intensity. The non-condensable gas faults that have the most negligible impact on system performance in the short term will reduce the cooling capacity by about 1.1% and the COP value within 3%. The refrigeration undercharge fault has a smaller impact on the system than the overcharge fault.

(2) The impact of simultaneous faults on VRF system performance is not a simple superposition of the impact of a single fault. Under simultaneous fault, faults will affect each other, significantly cancel or combine synergistically. For example, for VRF system performance, indoor fouling with outdoor fouling simultaneous fault has a noticeable superimposing effect, and the undercharge with outdoor fouling simultaneous fault has canceling effects. When the fault intensity of one of single fault is further increased, its superposition or cancel influence will gradually decrease.

(3) Some of the faults' effects on VRF system variables are similar, e.g., overcharge fault and outdoor fouling, undercharge fault, and indoor fouling. Correspondingly, the same simultaneous fault may lead to different variations due to the different fault intensity. This phenomenon is most typical for outdoor fouling with indoor fouling simultaneous fault. This is undoubtedly the difficulty of fault detection and diagnosis. Compressor discharge pressure feature can be used as a vital parameter indicator of whether the system is faulty. Condenser supercooling temperature feature can be used to identify the characteristic variables of refrigeration undercharge and indoor fouling faults in the system. Only the indoor fouling fault will cause a negative variation trend in the compressor suction temperature feature.

(4) In simultaneous fault, the influence of the fault on the variable trend is not only superimposed and offset, but also the trend influence of some faults has a dominant characteristic. The negative trend of discharge superheat temperature feature caused by the overcharge fault is a dominant characteristic. This means that if the outdoor fouling fault is included, the

simultaneous faults must cause a negative trend variation to the discharge superheat temperature feature.

Acknowledgements

The authors gratefully acknowledge the support of National Natural Science Foundation of China (Grant number 51876070 and 51906181).

References

[1] J.H. Wu, Z. Xu, F. Jiang, Analysis and development trends of Chinese energy efficiency standards for room air conditioners, Energy Policy, 125 (2019) 368-383.
[2] EIA, Annual Energy Outlook 2020 with projections to 2050, U.S. Energy Information Administration, Office of Energy Analysis, U.S. Department of Energy, (2020).
[3] J.Y. Liu, Y.P. Hu, H.X. Chen, J.Y. Wang, G.N. Li, W.J. Hu, A refrigerant charge fault detection method for variable refrigerant flow (VRF) air-conditioning systems, Applied Thermal Engineering, 107 (2016) 284-293.
[4] M. Kassai, Energy Performance Investigation of a Direct Expansion Ventilation Cooling System with a Heat Wheel, Energies, 12 (2019).
[5] M. Farzad, Modeling the effects of Refrigerant Charging on Air Conditioner Performance Characteristics For Three Expansion Devices, Dissertation Information Service, (1990).
[6] M. Farzad, D. O'Neal, System performance characteristics of an air conditioner over a range of charging conditions, International Journal of Refrigeration, 14 (1991) 321–328.
[7] D.Y. Goswami, G. Ek, M. Leung, C.K. Jotshi, S.A. Sherif, F. Colacino, Effect of refrigerant charge on the performance of air conditioning systems, International Journal Of Energy Research, 25 (2001) 741-750.
[8] Z. Du, P.A. Domanski, W.V. Payne, Effect of Common Faults on the Performance of Different Types of Vapor Compression Systems, Applied Thermal Engineering, 98 (2016) 61-72.
[9] J.B. Dooley, Effects of system cycling, evaporator airflow, and condenser coil fouling on the performance of residential split-system air conditioners, Texas A & M University, (2005).
[10] J.B. Chen, Simple rule-based methods for fault detection and diagnostics applied to packaged air conditioners / Discussion, ASHRAE Transactions, 107 (2001) p.847-857.
[11] M.S. Breuker, J.E. Braun, Common faults and their impacts for rooftop air conditioners, HVAC&R Research, 4 (1998) 303-318.
[12] N. US Department of Commerce, Heating Mode Performance Measurements For A Residential Heat Pump With Single-Faults Imposed, NIST TN - 1648.
[13] S.H. Yoon, W.V. Payne, P.A. Domanski, Residential heat pump heating performance with single faults imposed, Applied Thermal Engineering, 31 (2011) 765-771.
[14] M. Kim, W.V. Payne, P.A. Domanski, S.H. Yoon, C. Hermes, Performance of a residential heat pump operating in the cooling mode with single faults imposed, Applied Thermal Engineering, 29 (2009) 770-778.

[15] Y. Hu, D.P. Yuill, A. Ebrahimifakhar, A. Rooholghodos, An experimental study of the behavior of a high efficiency residential heat pump in cooling mode with common installation faults imposed, Applied Thermal Engineering, 184 (2021) 116116.
[16] B.C. Krafthefer, D.R. Rask, U. Bonne, Air-Conditioning and Heat Pump Operating Cost Savings by Maintaining Coil Cleanliness, (1987).
[17] D. Bultman, L. Burmeister, V. Bortone, Effects of Condenser Air Flow Blockage on Vapor-Compression Refrigerator Performance, Journal of Energy Resources Technology-transactions of The Asme - J ENERG RESOUR TECHNOL, 117 (1995) 349-353.
[18] B.C. Pak, E.A. Groll, J.E. Braun, Impact of fouling and cleaning on plate fin and spine fin heat exchanger performance, Ashrae Transactions 2005, Vol 111, Pt 1, 111 (2005) 496-504.
[19] A.H.H. Ali, I.M. Ismail, Evaporator air-side fouling: Effect on performance of room air conditioners and impact on indoor air quality, HVAC&R Research, 14 (2008) 209-219.
[20] B.A. Qureshi, S.M. Zubair, The impact of fouling on performance of a vapor compression refrigeration system with integrated mechanical sub-cooling system, Applied Energy, 92 (2012) 750-762.
[21] B.A. Qureshi, S.M. Zubair, The impact of fouling on the condenser of a vapor compression refrigeration system: An experimental observation, International Journal Of Refrigeration-Revue Internationale Du Froid, 38 (2014) 260-266.
[22] M.B. Bailey, System performance characteristics of a helical rotary screw air-cooled chiller operating over a range of refrigerant charge conditions, (1998).
[23] I.N. Grace, D. Datta, S.A. Tassou, Sensitivity of refrigeration system performance to charge levels and parameters for on-line leak detection, Applied Thermal Engineering, 25 (2005) 557-566.
[24] M. Mehrabi, D. Yuill, Generalized effects of refrigerant charge on normalized performance variables of air conditioners and heat pumps, International Journal Of Refrigeration-Revue Internationale Du Froid, 76 (2017) 367-384.
[25] Y. Hu, D.P. Yuill, S.A. Rooholghodos, A. Ebrahimifakhar, Y. Chen, Impacts of simultaneous operating faults on cooling performance of a high efficiency residential heat pump, Energy And Buildings, 242 (2021) 110975.
[26] H.L. Wan, T. Cao, Y.H. Hwang, S. Oh, A review of recent advancements of variable refrigerant flow air-conditioning systems, Applied Thermal Engineering, 169 (2020).
[27] Global Variable Refrigerant Flow (VRF) Systems Industry: Global Variable Refrigerant Flow (VRF) Systems Market to Reach $29 Billion by 2027. Amid the COVID-19 crisis, the global market for Variable Refrigerant Flow (VRF) Systems estimated at US$13, in: NASDAQ OMX's News Release Distribution Channel, New York, 2020.
[28] Z. Zhou, G. Li, H. Chen, H. Zhong, Fault diagnosis method for building VRF system based on convolutional neural network: Considering system defrosting process and sensor fault coupling, Building And Environment, 195 (2021) 107775.
[29] C. government, China Standard Service Network, in, 2021.
[30] G.N. Li, Y.P. Hu, H.X. Chen, J.Y. Wang, Y.B. Guo, J.Y. Liu, J. Li, Identification and isolation of outdoor fouling faults using only built-in sensors in variable refrigerant flow system: A data mining approach, Energy And Buildings, 146 (2017) 257-270.

[31] J. Meng, M. Liu, W. Zhang, R. Cao, Y. Li, H. Zhang, X. Gu, Y. Du, Y. Geng, Experimental investigation on cooling performance of multi-split variable refrigerant flow system with microchannel condenser under part load conditions, Applied Thermal Engineering, 81 (2015) 232-241.